2 *ortho*- and *ortho*-alternating-*para*-Phenylene Ethynylenes

2.1 Introduction

Arylene ethynylenes (AE) consist of aromatic rings connected via acetylene bridges. Most commonly is the class of phenylene ethynylenes (PE) where a benzene ring serves as aromatic moiety. But also incorporation of fused benzene ring systems and heteroaromatic systems such as anthracene and thiophene is common.[1] All these structures are relatively flat and rigid, and overall conformational flexibility is limited to rotation about few single bonds. Thus, packing and aggregation is a common phenomenon and potential control over secondary structure is facilitated. For example, stiff shape-persistent non-collapsing macrocycles are accessible that further stack into hollow nanotubes.[2]

Most reported AE-oligomers and polymers have structures with only one connectivity pattern, i.e. purely *para*-linked AEs resembling linear rods, linear *meta*-linked AEs often showing interesting conformational changes between extended zig-zag and helical shapes, or *ortho*-linked AEs usually in the form of macrocycles. Very few examples exist with structures of mixed connectivities, and those few all deal with either alternating or randomly distributed *para*- and *meta*-linkages forming the backbone. Strictly alternating P(*m*-alt-*p*PE)s[3] as well as P(*p*PE-alt-2,5-thiophene)s[4] were reported by the group of Pang, while Winter and Eisenbach described poly(AE)s with differing amounts of *meta*-kinks in the otherwise linear backbone.[5] The random incorporation of small amounts of *meta*-repeat units introduces kinks into the otherwise linear *p*PEs and dramatically increases solubility via introduction of conformational freedom while preserving the optical and electronic properties of linear conjugated *p*PE systems. Unsubstituted *para*- and *meta*-dibromobenzenes were also cross-coupled with *meta*-diethynylbenzene to give mostly insoluble and thus uncharacterized polymers.[6] Anderson reported on a series of 18 phenylene ethynylene pentamers displaying all possible combinations of *para*-, *meta*-, and *ortho*-linkages and their photoluminescence.[7]

Regular kinks in a linear PE strand can lead to a curved conformation of the planar backbone thus generating a helical structure (Figure 1). Depending on the regularity and the connectivity pattern of the kinks, a variety of potential helices with controlled dimensions is accessible, including tubular structures with defined cavities (e. g. *meta*-PEs) or π-conjugated and electrically conducting rod-like constructs (e. g. *ortho*-PEs). This interesting class of helical PEs is discussed in the following sections.

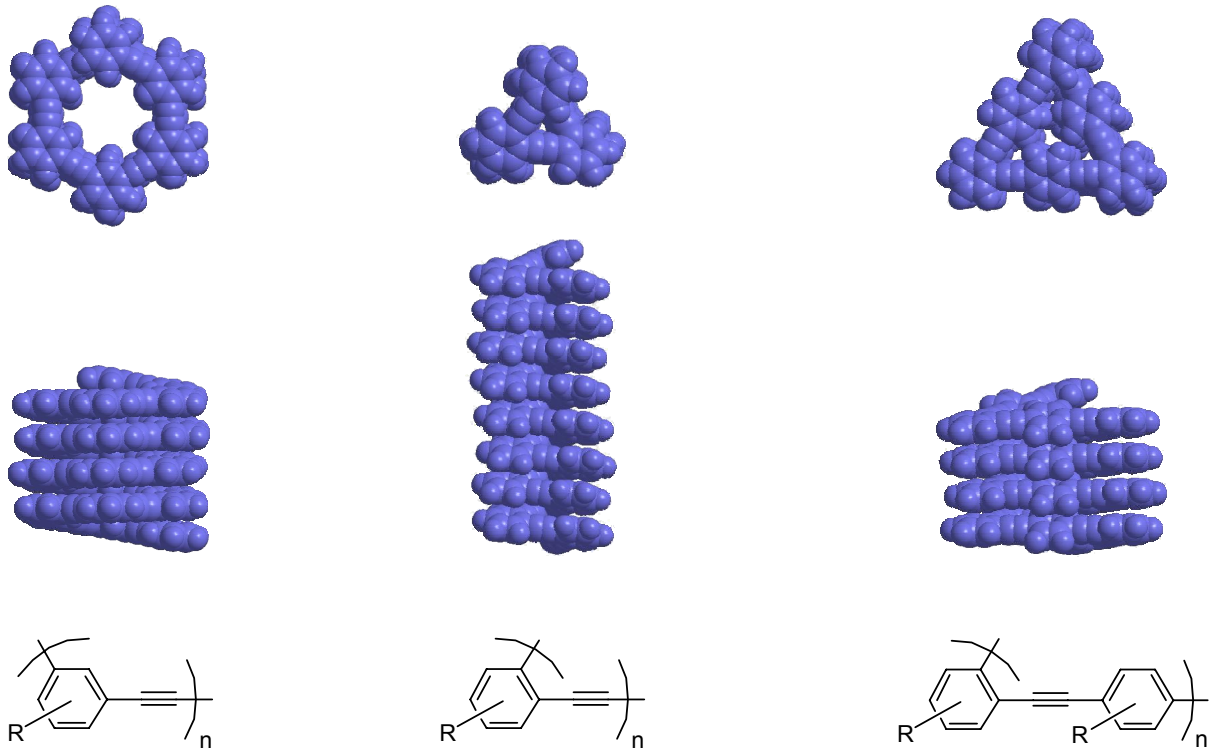

Figure 1: Diverse helical structures based on different connectivity of phenylene ethynylenes. Side chains on the models were omitted for clarity.

2.2 Known meta-Phenylene Ethynylene Oligomers and Polymers

An extensively studied class of synthetic foldamers constitute amphiphilic *meta*-connected phenylene ethynylene macromolecules displaying solvophobic driven folding. Inspired by Nature's exploitation of aromatic interactions and solvophobicity to generate and stabilize helical conformations among biomacromolecules, e. g. in the DNA double helix, Moore and coworkers published in 1997 a pioneering work on a series of amphiphilic *meta*-phenylene ethynylene oligomers (O*m*PEs, Figure 2, left).[8] The aromatic non-polar backbone (blue) carries polar tri(ethylene glycol) side chains (red) and therefore polar solvents lead to a segregation of the amphiphilic structure as the solvophobic regions hide from the solvent and adopt a compact shape with the polar side chains pointing towards the solvent. Because of the

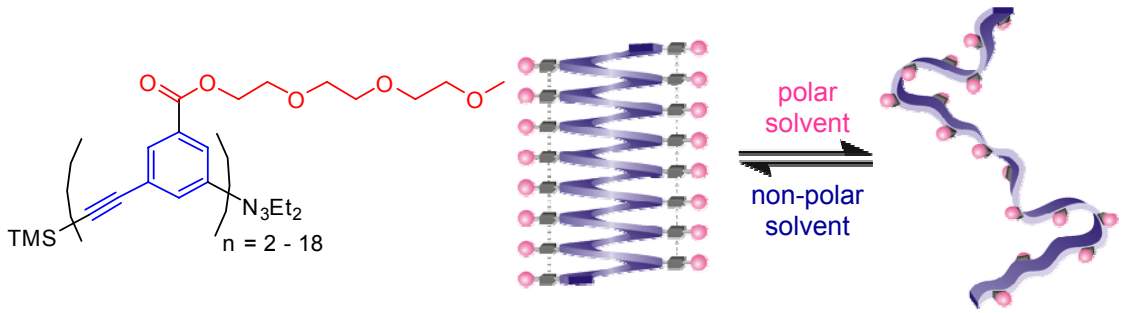

Figure 2: meta-Phenylene ethynylene oligomer family (left); solvophobic folding from random coil to helix (right).

restricted conformational freedom of the kinked *meta*-connectivity, the adopted compact structure is indeed a helix that is further stabilized by π-π-interactions between aromatic rings of adjacent turns. ESR studies with oligomers carrying spin labels demonstrated that each turn is comprised of approximately six repeat units[9] as expected from the hexagonal symmetry and bond angles of 120° between *meta*-substituents on a benzene ring. Due to the structure's rigidity and shape-persistence, a tubular cavity of approximately 7 Å in diameter is created upon folding into a helix.

Convenient optical monitoring of the folding process has been established for this type of backbone. While *cisoid* and *transoid* conformations differ in their absorption spectra, isolated and stacked cross-conjugated repeating units (i.e. *meta*-connected PEs) display direct and excimer-like emission, respectively. In addition, circular dichroism (CD) can be used as an alternative optical method, but only if (supramolecular) chirality is present.

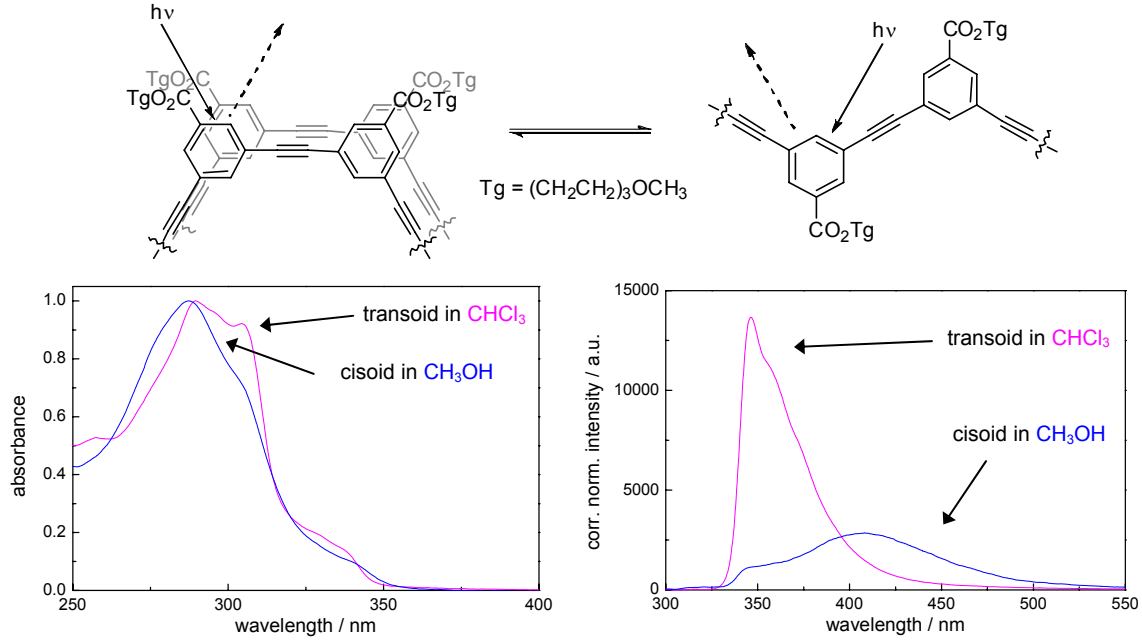

Figure 3: Transoid (left) and cisoid (right) conformations of meta-connected phenylene ethynylenes (top) reflecting the helix-coil transition and ist monitoring (bottom) by absorbance (left) and fluorescence (right).

A large variety of analogous helical foldamers has been synthesized derived from *m*PE, such as single-site modified oligo(*m*PE)s,[10] poly(*meta*-ethynylpyridine)s for saccharide binding,[11] imine-containing oligo(*m*PE)s for dynamic oligomerizations,[12] metal-bridged oligo(*m*PE),[13] amide carrying oligo(*m*PE)s for backbone-rigidification through hydrogen bonding,[14] and azo-containing oligo(*m*PE)s.[15]

The vast majority of publications are restricted to defined oligomers. A few polymer versions of helical *meta*-phenylene ethynylenes include cationic poly(*m*PE)s,[16] anionic poly(*m*PE)s,[17] and non-ionic poly(*m*PE)s.[18] In the last example, the Polysonogashira-

coupling was run with trimethylsilyl-protected acetylenes using an *in-situ* deprotection protocol[19] as described in Section 2.6.2. Polymer brushes and block copolymers based on *meta*-connected phenylene ethynylenes are presented in Chapter 3.

Besides the *meta*-connectivity, other linkage motifs are possible. While *para*-linked PEs represent stiff rods, *ortho*-linked phenylene ethynylenes (*o*PEs) possess the structural prerequisite for folding into a helix in a *cisoid*-conformation where three repeating units would form one turn. Here, the inner cavity of *mPE*-foldamers is discarded in favor of an increased aspect ratio and a π-conjugated backbone.

2.3 π-Conjugated Polymeric Foldamers

π-Conjugated polymers have potential applications as sensors,[20] as well as electronic and optoelectronic materials such as OLEDs and TFTs. The effective conjugation length (band gap) intrinsive to the nature of the backbone, conformation, and aggregation among others offer a wide variety to manipulate chemical and physical properties of this class of materials. A key feature is the secondary structure that dictates the three-dimensional conformation adopted by the polymer backbone either in solution or in the bulk, and therefore governs the overall material's properties. Especially intriguing is the helical motif, giving the polymer a tubular or rod-like shape, depending on the presence or absence, respectively, of an inner cavity. Studying, elucidating, and in the end controlling the secondary structure constitutes a major task among the field of organic and materials chemistry, as conjugated polymeric foldamers display promising features as, for example polarized emission due to the presence of macromolecular chirality.

There is not much published in the literature about π-conjugated helical polymers and most of those works deal with polyacetylenes[21] (Figure 4, left). Since 2003, three papers dealing with conjugated aromatic polymers appeared. First, the group Stamm reported on poly(alkylthiophene)s folding and aggregating in non-polar solvent mixtures into helical nanotubes.[22] Meijer and coworkers described the folding of chiral polythiophenes[23]

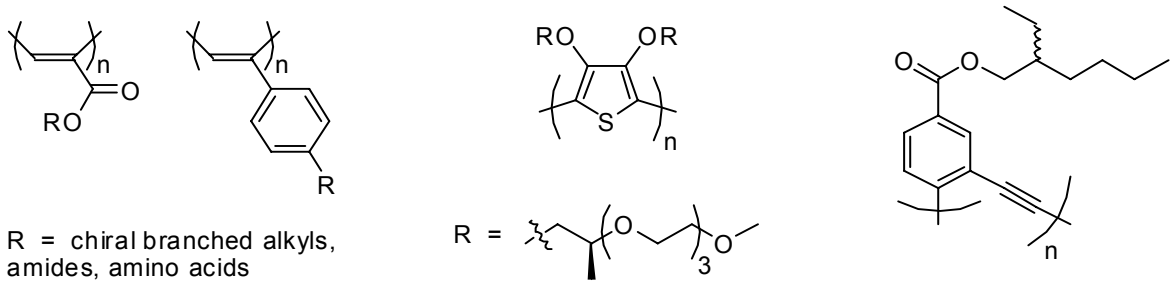

Figure 4: π-conjugated helical foldamers: polyacetylenes (left), polythiophenes (center), and poly(ortho-phenylene ethynylene)s (right).

(Figure 4, center). Folding was observed in water as the thiophenes carried tetra-ethylene glycol side chains and the authors conducted manifold studies to rule out aggregation. Although the side chains were optically active, they apparently failed to transfer their chirality to the aromatic backbone and no CD signal could be detected. The third paper was published by our group by Khan and Hecht[24] and dealt with poly(*ortho*-phenylene ethynylene)s (Figure 4, right) and reported on preliminary folding studies.

As conjugated polymer backbones tend to be relatively rigid, they are prone to aggregation, and distinguishing aggregation from helical folding represents a major effort when studying these kinds of structures. Concentration-dependent spectroscopic studies can reveal aggregation when non-linear relations, i. e. non-Lambert-Beer behavior, are found.

2.4 Known ortho-Phenylene Ethynylenes

The folding properties of *meta*-linked phenylene ethynylenes have been extensively studied and O*m*PEs represent an established field of research among foldamers. However, very few examples for *ortho*-connected analogues exist at all, and in only one case published by our group helical folding was studied.[24] Albeit strong distortions occur during folding due to the tight screwing of only three aromatic units per turn, theoretical studies support the possibility of solvophobically driven helical folding[25] although the planar zig-zag conformation constitutes the energetically preferred secondary structure.[26] Tew and coworkers reported on folding of a tetrameric *o*PE bearing polar side chains monitored by NMR,[27] somewhat extending the perception of folding as extended and helical conformations differ by a single bond rotation. Grubbs and Kratz synthesized a series of unsubstituted oligo(*o*PE)s, i.e. up to the nonamer and studied their spectroscopic properties.[28] Crystallization of the pentamer revealed a partially helical structure in the solid that hinted towards stabilizing aromatic π-π-interactions between the turn. Bunz and coworkers, in addition, reported on pyridine-capped O*o*PEs and their crystallization conformation.[29] The series up to the pentamer with two methoxy groups per repeat unit showed no helical packing in the solid. Otera and coworkers developed a synthetic route to *o*PE-oligomers up to the heptamer circumventing the Sonogashira-reaction step,[30] but no folding was studied, similar to Anderson, who synthesized an unsubstituted *o*PE-pentamer on a solid support.[7]

2.5 Novel OoPEs and P(o-alt-pPE)s

Apart from a preliminary report on folding poly(*ortho*-phenylene ethynylene)s,[24] no detailed study of helical conformations among these conjugated structures exist. Thus, a series of suitably substituted *o*PE-oligomers was synthesized (Figure 5, left). In order to use solvophobic driving forces for folding, amphiphilicity between the aromatic backbone and the side chains has to be generated and thus polar ethylene glycol chains will be attached via ester moieties to the repeating units. In addition, the connection via ester groups reduces the electron density in the aromatic backbone and presumably strengthens aromatic π-π-interactions,[31] thus further stabilizing potential helical conformations. Absorption as well as

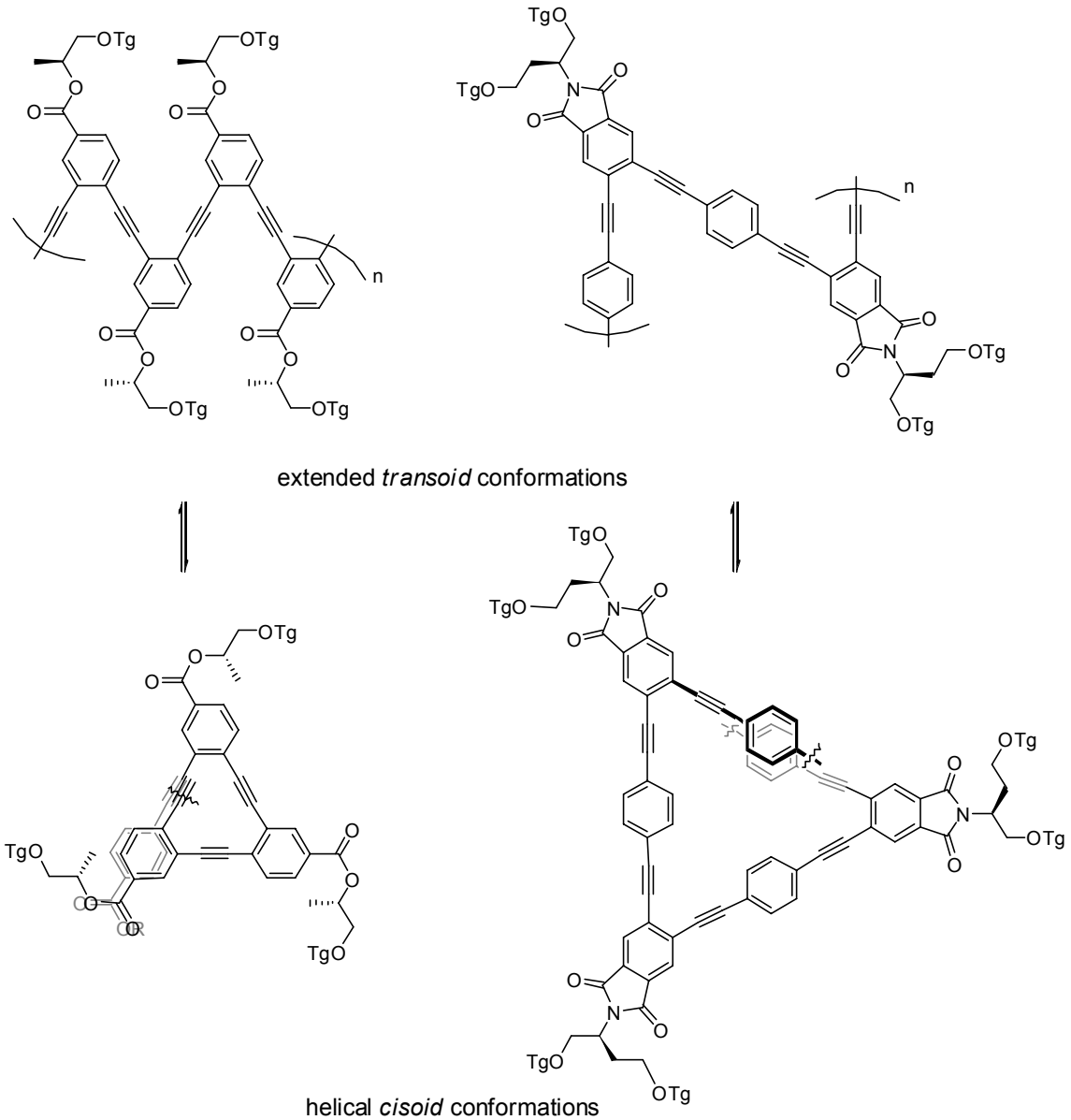

Figure 5: Targeted conjugated and potentially folding phenylene ethynylene architectures: extended transoid conformation (top) and helical cisoid conformation (bottom) of ortho-phenylene ethynylene (left) and ortho-alternating-para-phenylene ethynylene. Tg = –$(CH_2CH_2O)_3CH_3$.

fluorescence spectroscopy was used to elucidate structure-conformation correlations within the oligomer series in accordance to established work with *m*PEs. As optically active centers have been incorporated in the side chains, CD spectroscopy was additionally used, representing a powerful tool for demonstrating chiral superstructures like helical conformations. With O*m*PEs, folding was observed with minimal oligomer lengths of 10-12 repeating units, which resembles two full turns (Figure 6, blue). In the case of *ortho*-connected PEs, only three units are needed for a single turn and the higher enthalpic expense, due to a larger deviation from planarity, should be somewhat compensated by lower entropic demands when compared to the *m*PE-analogs, thus at approximately the stage of a hexamer folding-equivalent effects should begin to arise (Figure 6, red).

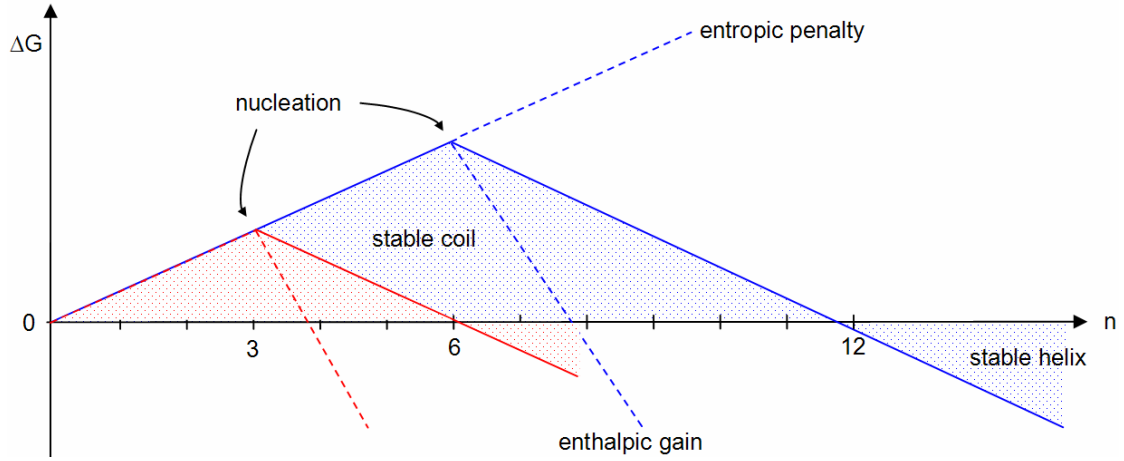

Figure 6: Interplay of entropic and enthalpic forces upon folding: The entropic cost of a folded conformation is compensated by stabilizing aromatic π-π-interactions arising the moment a full turn is achieved (nucleation) and fully compensated after ~2 turns (mPEs:12 r.u., blue; oPEs: 6 r.u., red).

To lower the required distortion of the aromatic rings when adopting a helical conformation, additional "spacers" were introduced into the structure in between *ortho*-PE units as depicted in Figure 5, right. Here, *ortho*-linked phenylene ethynylene units are alternating with unsubstituted *para*-connected phenylene ethynylene units. Now, six repeat units form a turn and the π-conjugation length along the backbone should be increased due to reduced torsion between aromatic units. As the *para*-units do not carry any solubilizing side chains, the *ortho*-substituted corner units were equipped with branched side chains for compensation. The side chains were linked to the backbone via an imide moiety instead of an ester to increase the total symmetry of the structure and provide an extended flat surface to enhance π-π-stacking. It should be noted, that a future side chain exchange is not possible as with ester moieties. Again, a chiral center was incorporated into the side chain to allow for monitoring by CD spectroscopy. In addition, in the folded state, the ^{1}H-NMR should discriminate inner and outer protons of the otherwise equivalent H's of the *para*-moiety, presenting an additional tool for studying folding processes.

2.6 Synthesis of ortho-Phenylene Ethynylenes

2.6.1 Synthetic Approaches: Iterative Divergent/Convergent Synthesis, Oligomerization, Synthesis on Soluble Support

Many different approaches for the synthesis of defined oligomers of any kind have been established.[32] Independent from the synthetic methodology, a trifunctional monomer with orthogonal protecting groups is always required. For our oligo(*o*PE)s, the ester moiety of a benzoate was used for carrying the solubilizing chain. The aromatic backbone was constructed by palladium and copper catalyzed Sonogashira cross-coupling steps, thus protecting groups for aryl iodide and terminal acetylene groups were introduced in the form of the triazene moiety and the trimethylsilyl (TMS) group, respectively.

Classic aromatic amine-halogen transformations use the Sandmeyer reaction based on diazonium salts. The less frequently used triazene group resembles a superior form of the diazonium salt when targeting aryl halides, as it is stable to air, humidity, bases, and nucleophiles, and it can be used as a masking group for iodides as it tolerates many reaction conditions and can be purified by standard methods. Different methods are reported for transforming a triazene into an iodo function, such as acidic decomposition of the triazene in the presence of iodide salts[33] or using molecular iodine at elevated temperatures.[34] Here, the conversion with methyl iodide under high temperatures and pressure is applied as a general and versatile method for all kind of aromatic triazene compounds. As the reaction conditions are relatively harsh and molecular oxygen strongly inhibits the transformation, the mechanism is presumably radical and starts with the methylation of the terminal nitrogen of the triazene group (Scheme 1). Besides the desired aryl iodide, also molecular nitrogen and tetraalkylamonium iodide are generated.

The removal of the silyl group is well established and can be done either under basic conditions (K_2CO_3) or with fluorides (TBAF).[35] In both cases, the strongly exothermic formation of Si-O and Si-F bonds, respectively, acts as driving force.

Three differing approaches to a series of *ortho*-phenylene ethynylene oligomers are presented in the following sections. The iterative divergent/convergent procedure leads quickly to longer oligomers of defined length as the number of repeating units is doubled with

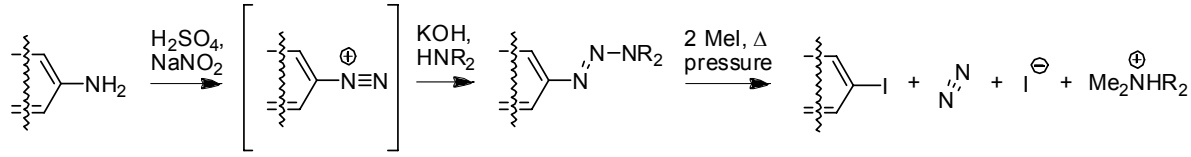

Scheme 1: Generation of the triazene group and its transformation into an iodide.

every activation and coupling cycle (Section 2.6.4). Bidirectional growth, either in solution or on a polymeric support, relays on a central repeating unit carrying two identical functional groups to where building blocks with complementary functional groups are attached-to. But this procedure is ruled out because of inadequate symmetry of *ortho*-phenylene ethynylenes. The oligomerization of short oligomers represents a compromise between purely step-by-step approaches that deliver defined oligomers under extensive investment of time and synthetic work and a polymeric approach yielding an inseparable mixture of a wide range of oligomers out from a monomer building block. For example, the synthesis of a reactive tetramer requires moderate effort and after oligomerization, the separation of the obtained octamer, dodecamer, hexadecamer etc. can be accomplished as their molar masses and properties differ largely. Thus, this approach allows to significantly speed up the generation of oligomers series (Section 2.6.5). The liquid phase approach is related to Merrifield's[36] solid-support synthesis and possesses its own advantages and disadvantages and will be discussed thoroughly in Section 2.6.6.

2.6.2 The Sonogashira Cross-Coupling Reaction

The Sonogashira – also called Sonogashira-Hagihara – cross coupling reaction[37] belongs to the steadily growing and nowadays indispensable transition metal-catalyzed cross-coupling reactions. Aryl halides are cross-coupled with terminal acetylenes to generate an arylene-ethynylene bond. The arene building block includes many classes of aromatic and heteroaromatic rings, as benzenes, fused aromatic ring systems, pyridines, thiophenes, or pyrrols. The halide moiety can be bromide or iodide, but also pseudo-halides as triflates, tosylates or mesylates. The coupling mechanism involves two catalytic cycles, the palladium and the copper cycle.[38]

The active catalytic species is presumably Pd^0L_2. Used are Pd^0-catalysts with phosphine ligands, by far the most common – and also used in this work – is $Pd(PPh_3)_4$. Easier to handle are Pd^{II}-salts; here, the Pd^0-species is generated *in-situ* by oxidative homocoupling of two terminal acetylenes thus altering stochiometry of reactants (Figure 7, a). These diines represent a major sideproduct in Sonogashira reactions and their formation occurs when e. g. traces of oxygen oxidize the sensitive Pd^0-species to Pd^{II} besides the oxidative Cu-catalyzed Glaser coupling, thus degassed solvents and reactants are used. Another side reaction consists in the dehalogenation of aryl halide adducts via hydride transfer from the palladium complex, a phenomenon increasing at higher temperatures.

The catalytic cycle starts with oxidative insertion of palladium into the arene-halogen bond (Figure 7, b), facilitated by electron withdrawing substituents at the aromatic ring. Using aryl

iodides, the insertion occurs smoothly at room temperature, while couplings with aryl bromides require higher temperatures and might lead to increasing amounts of side reactions.

In the second step, the so-called transmetalation, a before generated ethynyl cuprate exchanges its metal center for the palladium and thus replaces the halide at the Pd^{II}-complex (Figure 7, c). In the last step, aryl and ethynyl ligands are rearranged around the metal center to mutual vicinity and eliminated as the ethynyl arene condensation product regenerating the Pd^{0}-species (Figure 7, d and e, respectively, "reductive elimination"-step).

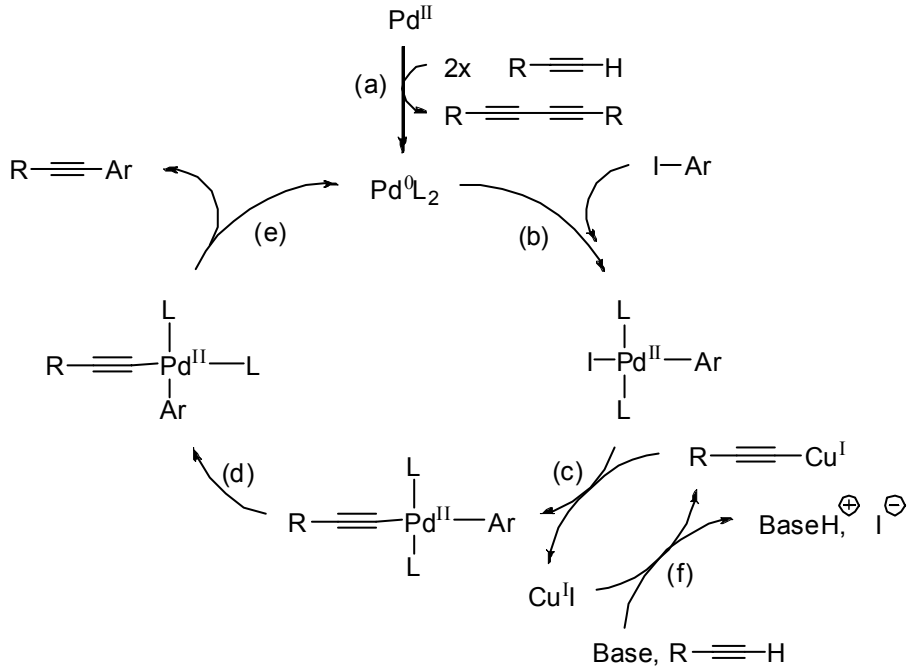

Figure 7: Catalytic cycle of the Sonogashira-cross coupling reaction for condensing aryl halides with terminal acetylenes. Central palladium cycle includes oxidative insertion (b), transmetalation (c), cis-trans-rearrangement (d), reductive elimination steps (e). Included are the palladium activation via diacetylene formation (a) and copper regeneration cycle (c, f).

Interwoven to the above described palladium cycle runs the copper cycle. The terminal acetylene is converted into the corresponding cuprate and the released proton is trapped by the base (Figure 7, f), in general an organic amine. After the transmetalation step, copper iodide is regenerated and enters a new catalytic cycle.

Water itself does not interfere in the Sonogashira reaction, but if adducts are prone to saponification, all components and especially the solvents have to be dry, as large amounts of base are present during the reaction.

In the literature, Sonogashira couplings without copper are also often reported,[39, 40] as well as couplings under aerobic conditions,[39, 41] couplings replacing Pd with nickel,[42] and Sonogashira protocols using silyl-protected acetylenes that are deprotected *in-situ*.[19] In the latter case, DBU is used as a base in combination with defined amounts of water to remove the silyl group from the acetylene prior to Sonogashira condensation. Thus, the concentration

of free acetylenes is kept low and diine formation is minimized down to an undetectable level. In this case, obviously no dry solvents are required.

2.6.3 Monomer Synthesis

Synthesis of the orthogonally protected monomer building block **4** starts with commercially available ethyl 4-aminobenzoate **1**. Bromination with NBS[43] provides aryl bromide **2** with the desired regioselectivity as both the electron-rich amine and electron-deficient ester direct the attacking electrophile into the 3-positionThe generated side product succinimide is easily removed by precipitation in many non-polar solvents.

Triazene formation[33, 44] follows a two-step one-pot protocol, first the diazonium salt is generated from the aniline and subsequent addition of a secondary amine yields the desired adduct **3**. Different secondary amines can be used for generating the triazene moieties: In this work, either pyrrolidine or diethylamine were used. When using the cyclic amine, corresponding products can be purified by recrystallization whereas diethyl triazenes could be more readily converted into iodides.

Sonogashira cross-coupling (see Section 2.6.2) of the aryl bromide with TMS-acetylene (TMSA) finally leads to the trifunctional monomer **4**. Elevated temperatures due to the bromine functionality and an excess of acetylene increase conversion and yield. The deoxygenation procedure by freeze-pump-thaw-cycles had to be altered in order to prevent evaporation of volatile TMS-acetylene.[45]

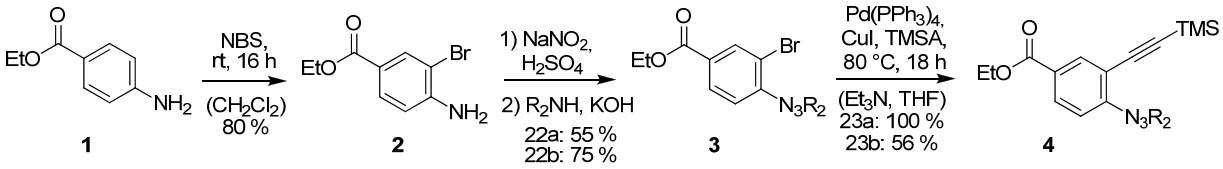

Scheme 2: Synthesis of ortho-phenylene ethynylene monomer.
a: $R_2NH = Et_2NH$, b: R_2NH = pyrrolidine.

For all Sonogashira couplings in this work, a Pd^0 catalyst was employed. We restricted the great variety of available catalysts to the standard catalyst tetrakis(triphenylphosphine)palladium $Pd(PPh_3)_4$ due to its versatility as well as rapid and easy accessibility. The catalyst preparation consists in a one-step synthesis that involves the injection of hydrazine to a hot solution of commercially available $PdCl_2$ and PPh_3 in DMSO resulting in a reduction of the palladium species under evolution of molecular nitrogen gas and precipitation of the yellow palladium catalyst upon cooling.[46]

2.6.4 Iterative Divergent/Convergent Synthesis

2.6.4.1 Synthesis

Key compounds are orthogonally protected building blocks that allow convergent activation/deprotection reactions for repetitive binomial divergent-convergent steps. The synthetic route to *o*PE oligomers starts with monomer **4** (Scheme 3). Selective activation of the triazene to aryl iodide **5** is achieved with neat methyl iodide at high temperatures and under (undefined) pressure.

The desilylation of **4** leads to the unprotected ethynylbenzoate **6**. Applied protocols include the desilylation with carbonates under mild conditions in the presence of water, but longer reaction times and sometimes slightly elevated temperatures are required, thus leading to partial saponification among ester-rich substrates. When methanol was used as the protic solvent, partial transesterification of the ethyl ester to the methyl ester was sometimes observed. In contrast, the deprotection with fluorides is extremely fast and leads to complete conversion within minutes but yields undefined byproducts and often necessitates purification by column chromatography.

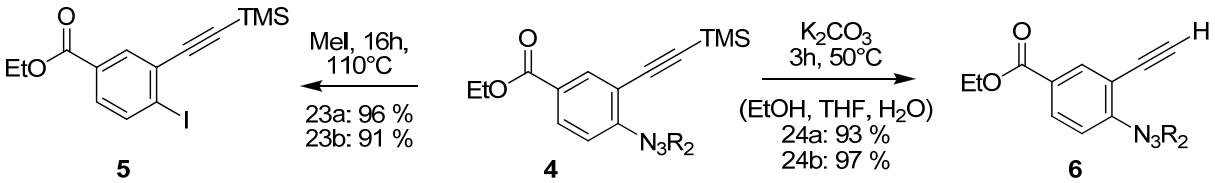

5 **4** **6**

Scheme 3: Selective activation/deprotection of monomer building block; a: R_2 = Et_2, b: R_2 = cC_4H_8.

Aryl iodides and terminal acetylenes are condensed via Sonogashira-cross coupling yielding the corresponding dimer **8** carrying again the two desired orthogonal protecting groups (Scheme 4). Several approaches were run but conversions were always relatively low and remaining starting material had to be removed by time-consuming column chromatography, as product, starting materials, and other byproducts had similar R_f-values. Already at this stage, problems with Sonogashira couplings involving *ortho*-substituted aryl iodides were eminent. Furthermore, the side chain should have been exchanged at the level of monomer synthesis, thus increasing the polarity difference between shorter starting materials and longer product and facilitating separation.

Subsequent activation or deprotection, respectively, of **8** afforded iododimer **9** and ethynyl dimer **7** in very good yields (Scheme 4). Again, their coupling to the corresponding tetramer was associated with unsatisfying yields, which even after tuning reaction parameters, e. g. temperature, solvent composition, and stochiometry could not significantly be improved.

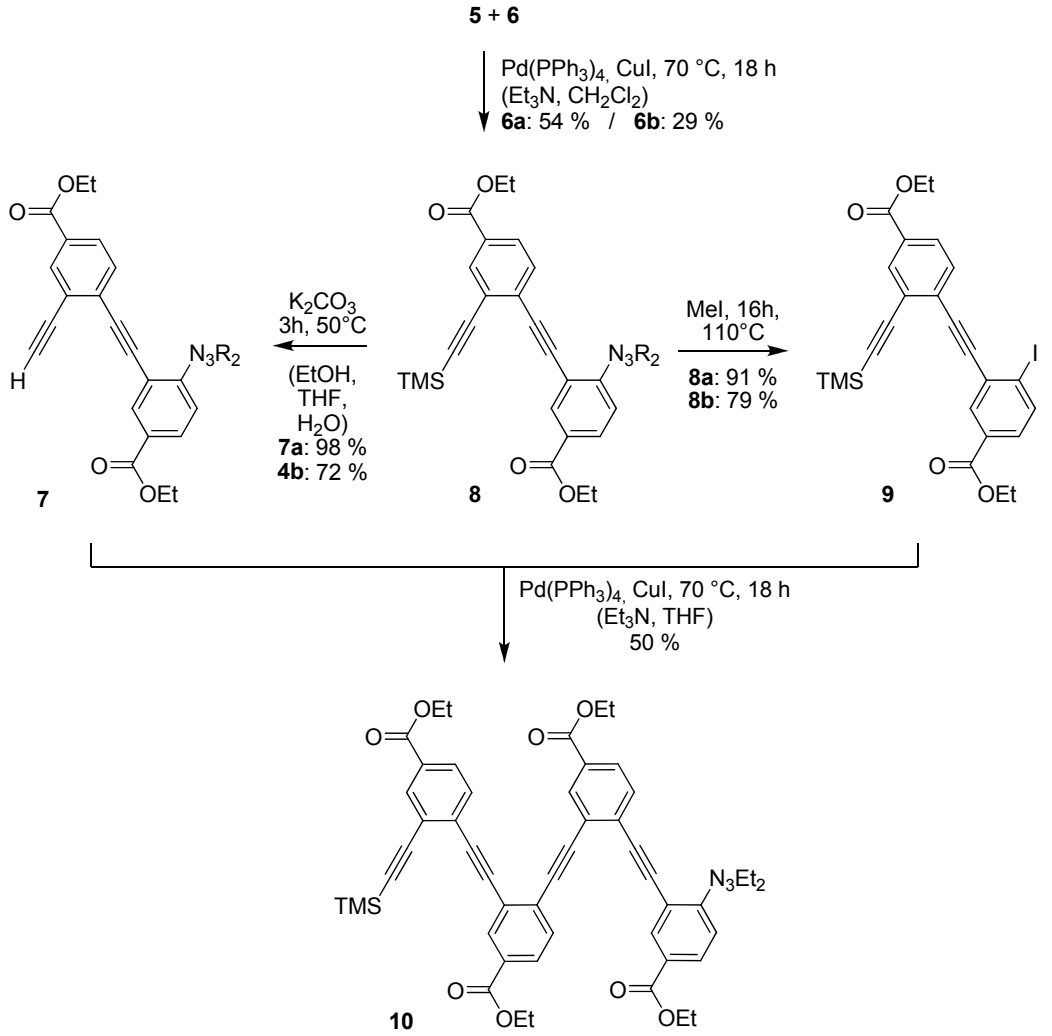

Scheme 4: Activation/deprotection and cross-coupling of ortho-phenylene ethynylenes; a: $R_2 = Et_2$, b: $R_2 = cC_4H_8$.

A critical aspect in optical spectroscopy is the influence of the end groups of oligomers, especially the triazene group would be active in the UV/vis and thus, both termini of the tetramer were subsequently activated and sealed with monofunctionalized cappers. The iodo-capper ethyl *para*-iodobenzoate was commercially available, while the *meta*-ethynyl-capper had to be synthesized. Thus, ethynyl benzoate carrying either a bromo- or an iodo-functionality in *meta*-position was cross-coupled with an excess of TMSA to yield the protected phenylene ethynylene **12** (Scheme 5). The silyl group was removed by either K_2CO_3 or TBAF and both options provided the free-acetylene capper in excellent yields.

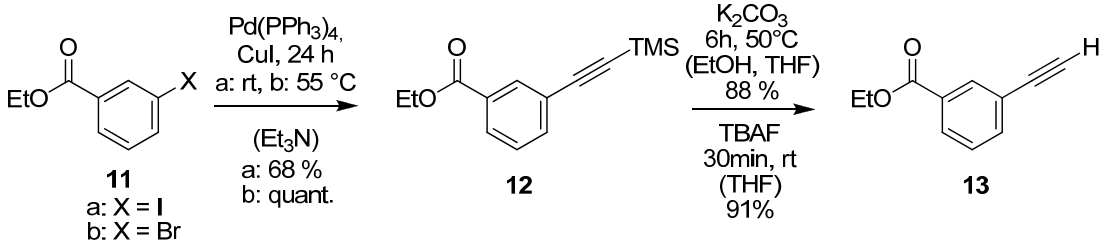

Scheme 5: Three-step route to free-acetylene capper.

As triazene-iodo transformations were in general more challenging than the desilylations, the generation of the iodo functionality was carried out first on the tetramer **10** and was achieved in surprisingly high yields (Scheme 6). Mono-activated tetramer **14** was cross-coupled with an excess of acetylene capper **13** to yield pentamer **15**. At this point, the Sonogashira coupling with iodo-benzoate capper was carried out using the TMS *in-situ* deprotection protocol. In the MS spectra of the product mixture no starting material was found and some signals might be attributed to partially saponified hexamer, but no useful amount of the hexamer was isolated.

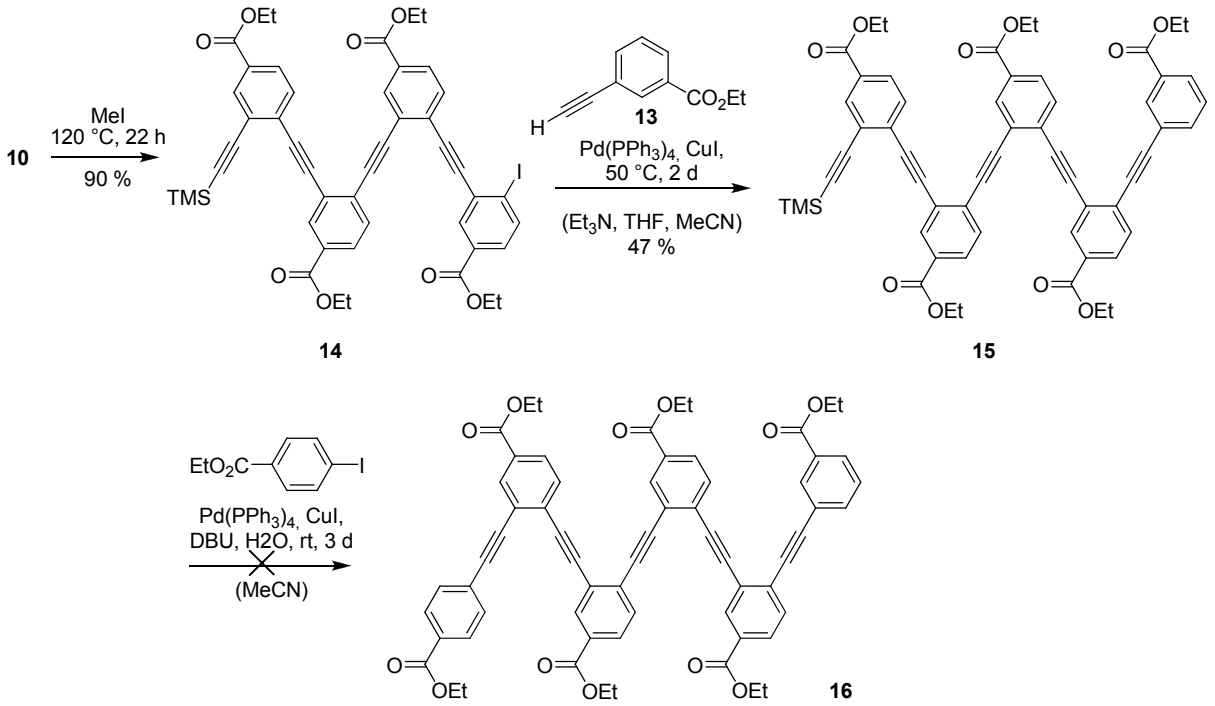

Scheme 6: Synthetic route to ortho-phenylene ethynylene hexamer via subsequent triazene activation and desilylation steps

Finally the envisioned hexamer was synthesized in reversed order steps, i.e. first, the silyl group – the more labile of both protecting groups – was removed in nearly quantitative yield with TBAF to give **17** (Scheme 7). Higher oligomers with several ester groups like this tetramer were not desilylated with potassium carbonate to avoid partial saponification of the esters. Sonogashira coupling with an excess of ethyl *para*-iodobenzoate gave pentamer **18** in satisfactory yields. The following triazene-iodo transformation gave enough material to finish the synthetic route. With larger molecular structures, these activations gave poorer and less reproducible conversions and yields: The absence of the silyl group minimized byproduct formation, but conversion was still low and significant amounts of starting material could be reisolated. Due to the experimental setup using a presurable glass apparatus without manometer, the reaction course resembles a black box: as the exact reaction pressure – an important parameter in this reaction – remains completely unrevealed no setup-yield

correlation was elucidated. Parameters influencing the reaction pressure are – besides temperature – the solvent volume, available gas volume, and the concentration. Concentrations were kept around 0.1 mol/L, otherwise N_2 gas generated during the reaction pushes pressure too high, and the glass vessel eventually explodes. The use of excess of ethyl *para*-iodobenzoate and **13** at the corresponding coupling steps gave far better yields among these difficult Sonogashira coupling reactions and thus negative effects of steric and electronic hindrance could be partially compensated.

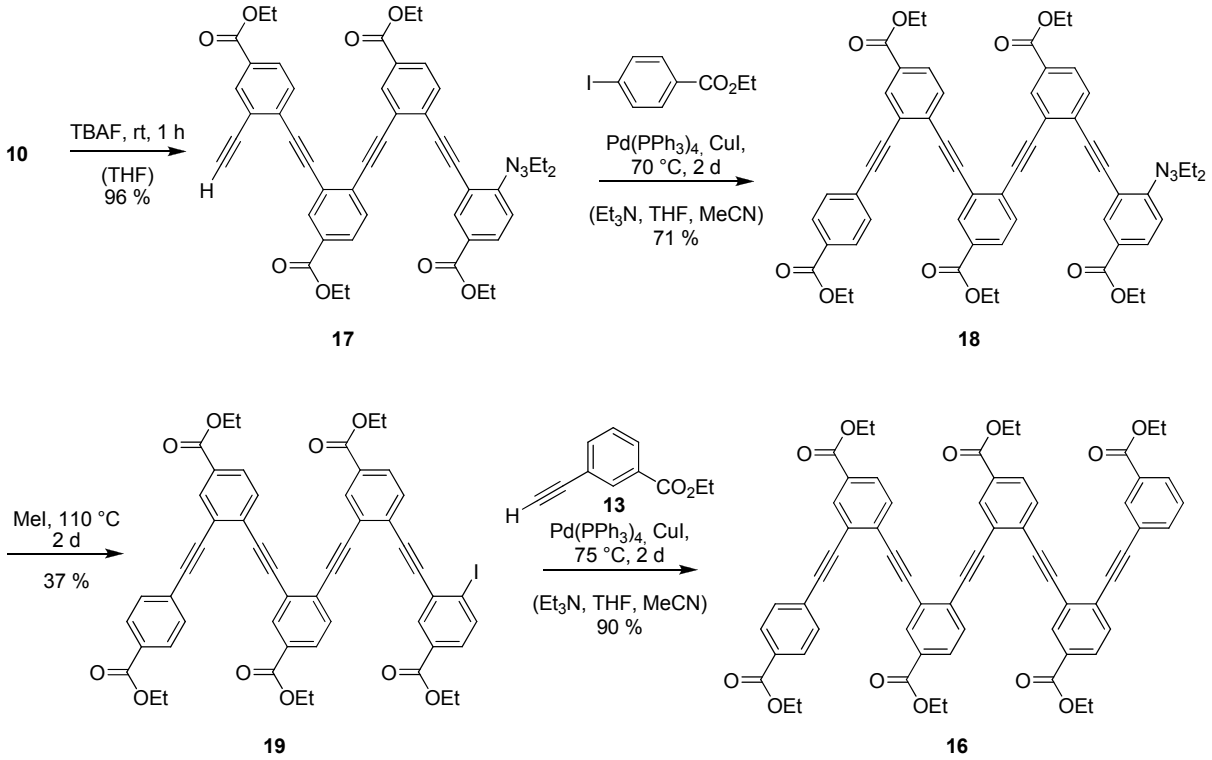

Scheme 7: Successful synthetic route to ortho-phenylene ethynylene hexamer via subsequent desilylation and triazene activation steps.

At the same time, a 3+3 approach was pursued: starting from reactive dimers **9** and **7**, the free-ethynyl-dimer was cross-coupled with excess of ethylene *para*-iodobenzoate, and the iododimer was coupled with excess of capper **13**. While facile deprotection of the TMS-acetylene on trimer **22** afforded **23**, the activation of the triazene on **20** was surprisingly difficult. With several atempts only small amounts of starting material could be converted into the aryl iodide, and separation was difficult yielding insufficient material to try the final condensation to the hexamer **16**.

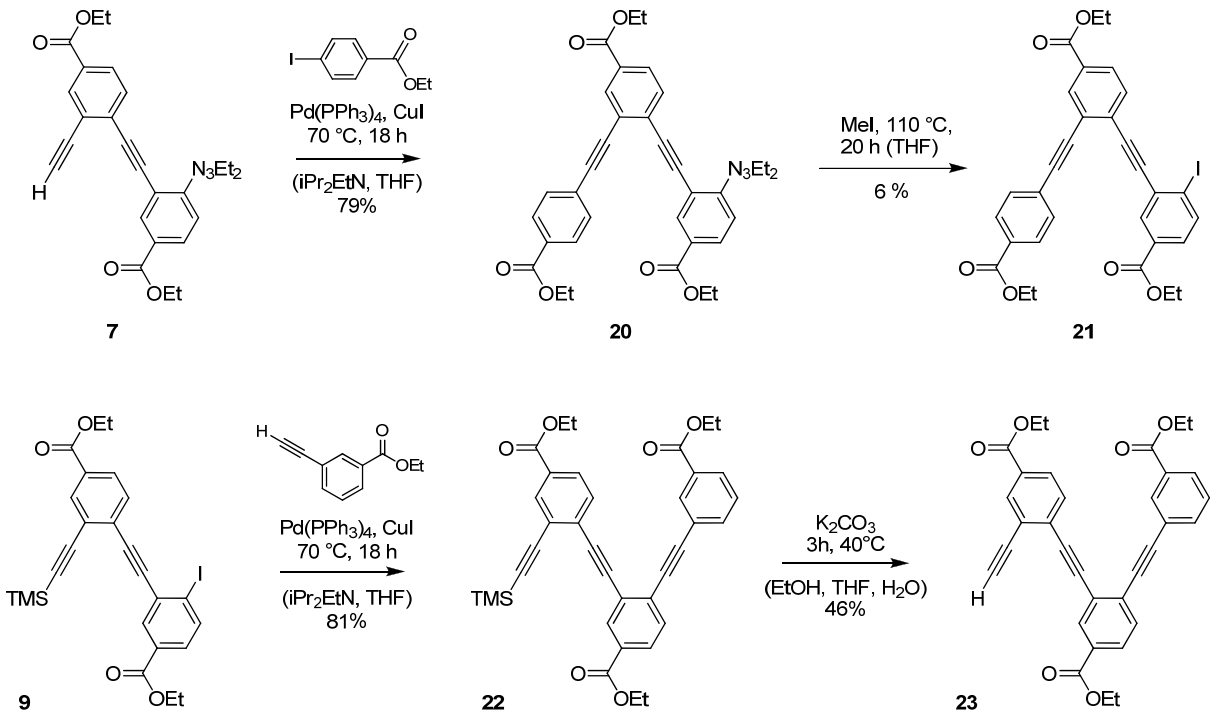

Scheme 8: Synthesis of complementary monofunctional ortho-phenylene ethynylene trimers.

An adequate exchange of the ethyl side chain on *o*PE-hexamer **16** not only increases solubility but also allows formation of layers on surfaces, if long alkyl chains are introduced, as well as solvophobic-driven folding, if amphiphilicity is introduced with the new side chain. A dodecyl chain was chosen to fulfill these two requirements. The hexamer **16** was reacted with a large excess of dodecyl alcohol employing potassium carbonate as the catalytic base. The reaction was run strictly water-free to prevent saponification, i.e. generation of unreactive carboxylate groups, and under reduced pressure to continuously remove ethanol generated during the reaction course. The crude product was isolated by precipitation in methanol, where excess dodecyl alcohol stayed in solution, and submitted again to the same procedure to drive transesterification to completeness, as monitored by MS and ^{1}H-NMR.

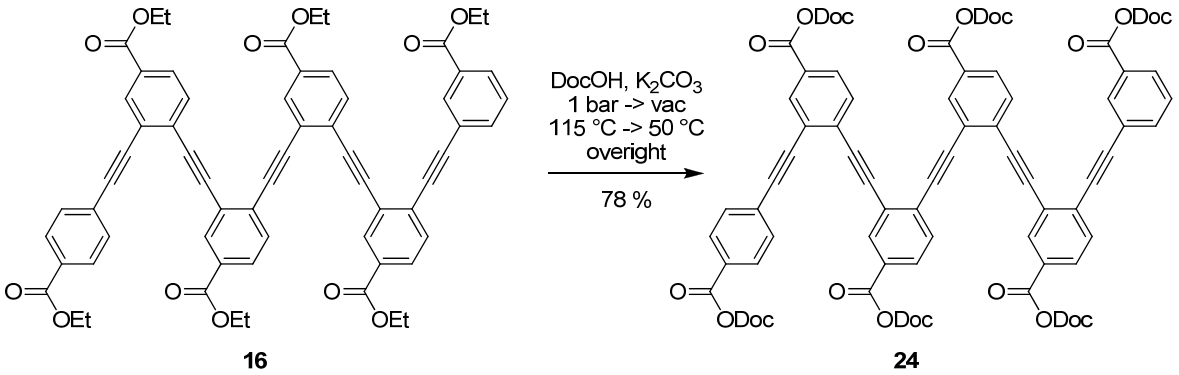

Scheme 9: Side chain exchange on ortho-phenylene ethynylene hexamer; Doc = $nC_{12}H_{25}$.

2.6.4.2 NMR and STM Results

The *ortho*-connected phenylene ethynylene hexamer possesses a structure pleasing to the eye, but lacks symmetry, and this fact complicated synthesis and leads to complex yet diagnosable NMR spectra. The ^{1}H-NMR spectrum of hexamer **16** is depicted in Figure 8. Almost every proton of the aromatic backbone (and many of the remaining ones) can be resolved and the splitting pattern in the spectrum is helpful for assigning the signals.

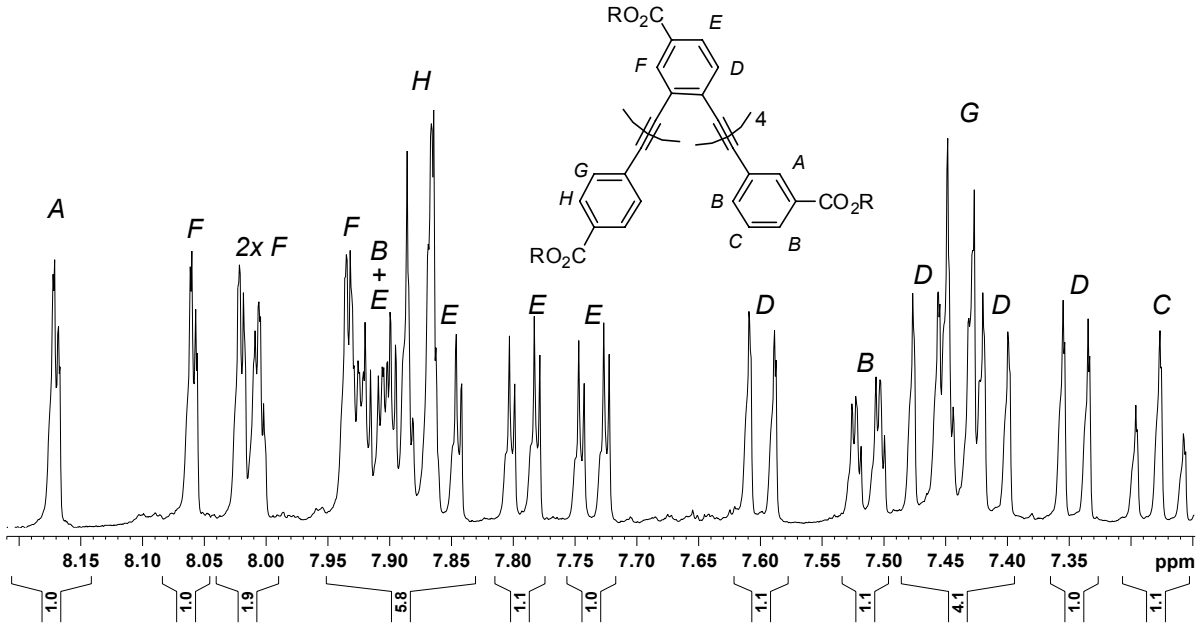

*Figure 8: ^{1}H-NMR spectrum of ortho-phenylene ethynylene hexamer **16** in $CDCl_3$ with partial assignment of signals by comparison with preceding molecular structures and with COSY-NMR (not shown). Magnified aromatic region is shown.*

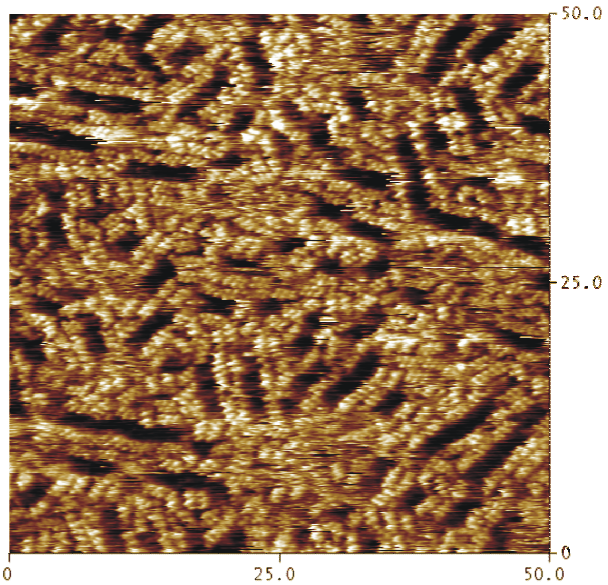

*Figure 9: STM-image of hexamer **24** on HOPG. Single and double rows of aligned extended hexamers can be recognized.*

In cooperation with the group of Prof. Jürgen Rabe at the Humboldt Universität zu Berlin, STM images of the hexamer carrying dodecyl side chains were recorded. This class of aromatic structures in their zig-zag conformation should form extended self-assembled monolayers that might allow to deduce conformational behavior and aggregation modes. In this case, a highly ordered pyrolytic graphite (HOPG) surface was used and long alkyl chains were introduced into the hexamer to allow for strong adsorption of the hydrocarbons to the graphite surface and thus prevent thermal motion and facilitate monolayer formation.[47] Figure 9 shows a representative STM image of the hexamer **24**. Ordered areas show structures of single and double rows of hexamers aligned along their length axis. How exactly these patterns of rows are generated and the mechanism and dynamics of their formation is still being investigated.

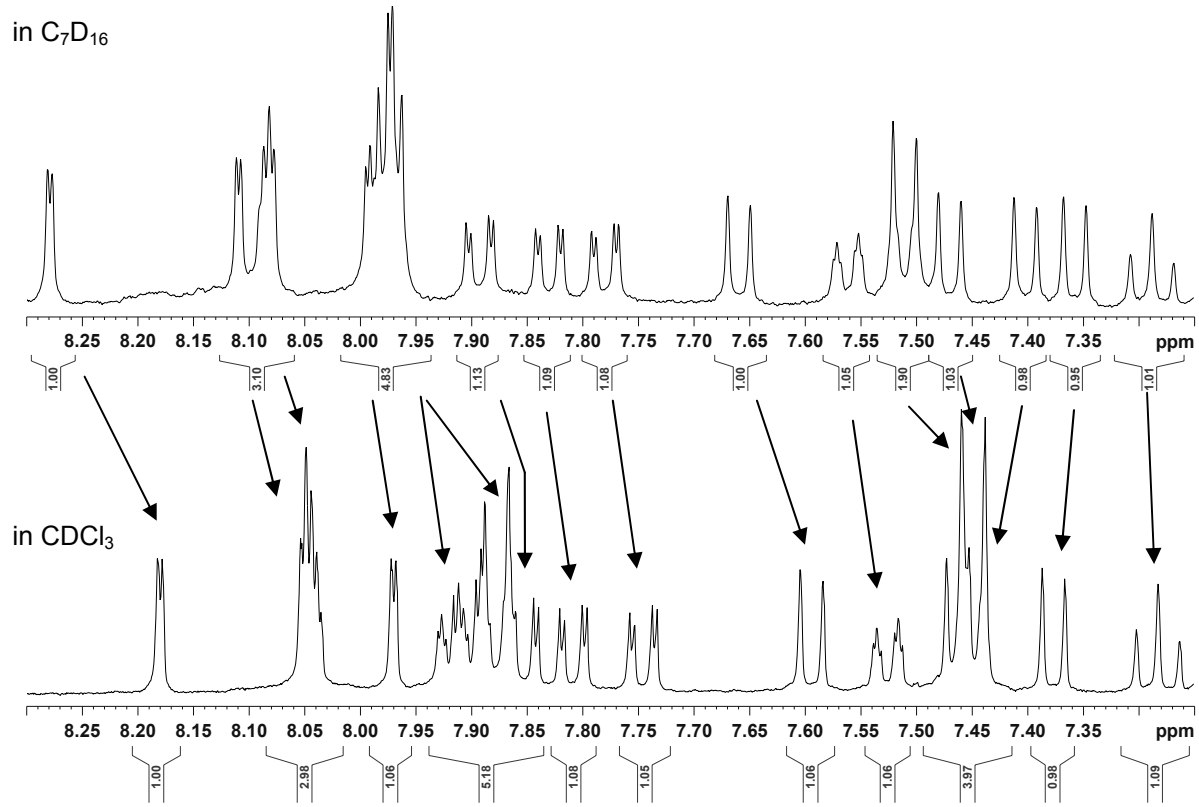

Figure 10: ^{1}H-NMR spectra of ortho-phenylene ethynylene hexamer carrying dodecyl side chains in C_7D_{16} (top) and $CDCl_3$ (bottom). Shown is the magnified region of aromatic signals.

Figure 9 shows the aromatic region of ^{1}H-NMR spectra of **24** in C_7D_{16} and $CDCl_3$. The differing shifts of the signals – while some do not shift – might be interpreted as conformational rearrangement of the aromatic backbone and not only as arising from solvent dipole interactions. Additional ^{1}H-^{1}H-NOESY NMR experiments should give further evidence for a helical conformation of the hexamer backbone via H-H contacts between protons of stacking aromatic rings.

2.6.5 Oligomerization of Tetramer

2.6.5.1 Synthesis and Separation

In order to gain access to higher oligomers and circumvent the difficult and low-yielding synthetic split-pool steps of activation/coupling and purification, an oligomerization of a suitable tetramer was studied. The *ortho*-phenylene ethynylene tetramer **14** carrying ethyl chains was subjected to a side chain exchange. The tetramer was dissolved in a large excess of enantiopure tetraglyme monomethylether alcohol **97**[48] and potassium carbonate added. The reaction was run in the strict absence of water to prevent saponification, i.e. generation of unreactive carboxylate groups on the tetramer. The reaction mixture was heated and pressure slowly reduced over several hours to remove generated ethanol from the reaction equilibrium. The exchange ran completely and the desired tetramer **25** (Scheme 10) was purified by three consecutive chromatography steps to remove excess tetraglyme alcohol that ran similar to the product. The TMS group was also removed during the side chain exchange, thus generating the reactive macromonomer carrying both complementary functional groups for Sonogashira couplings. The Polysonogashira condensations were run at high dilutions and for short times in order to stop the reaction at the stage of oligomers.

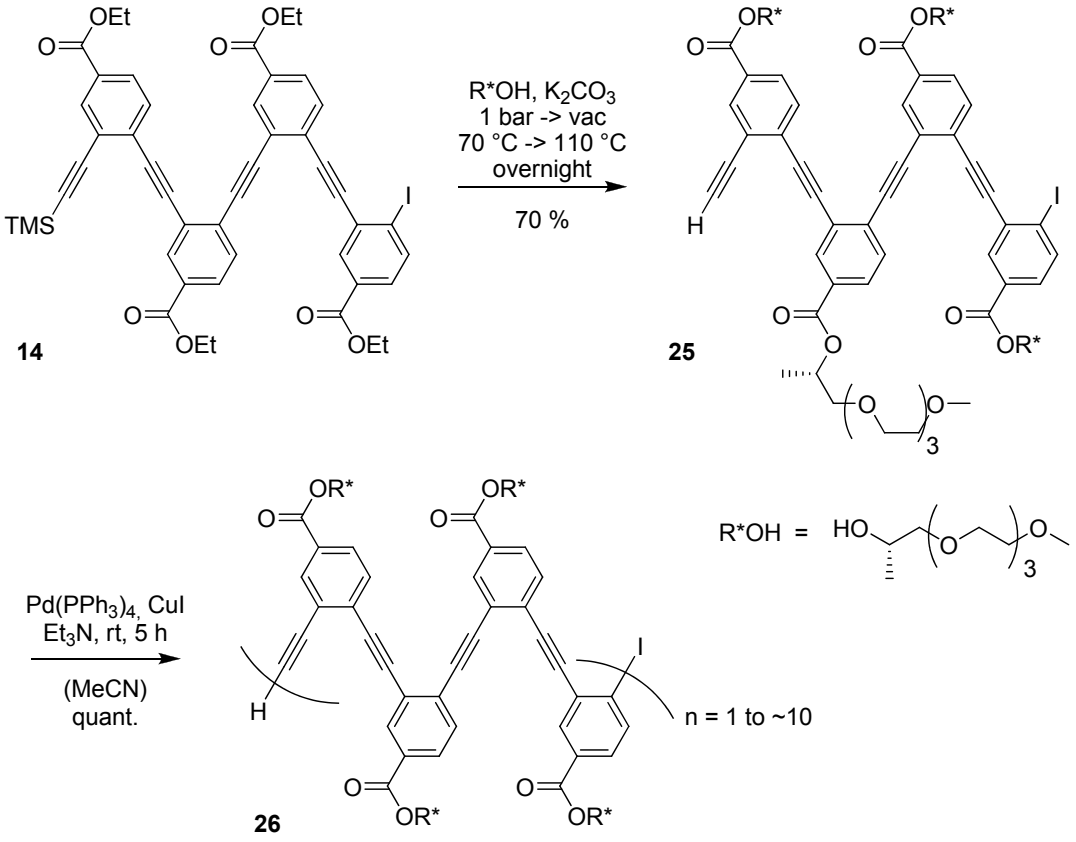

Figure 10: Synthesis of appropriate ortho-phenylene ethynylene tetramer and its oligomerization.

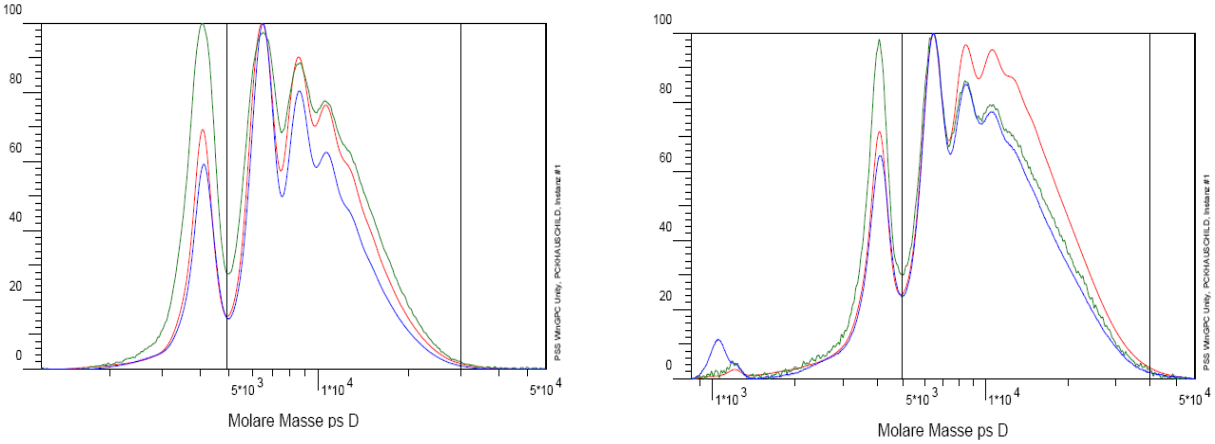

Figure 11: GPC traces of oligomerization of oPE-tetramer (THF); short time and diluted (left) and long time and concentrated (right); used detectors: UV 230nm (red), UV 280nm (green), RI (blue).

Different reaction conditions were tried in order to achieve an optimum amount of short oligomers (8 - 16 aromatic repeating units, i.e. n = 2 - 4). Figure 11 shows two GPC traces of such oligomeric mixtures. The reaction times were varied from 4.5 hours (left) to two days (right) and from concentrations of 0.007 mol/L (left) to 0.03 mol/L (right) while keeping all other parameters constant (solvents, temperatures, catalysts loadings). As can be seen from the figure, the differences for both extreme variants are moderate; after two days the tetramer is still present in the mixture while the amount of higher oligomers slightly increased and the polymer flank became more pronounced. Apparently, after a few hours the polymerization is finished and can not be pushed further to higher conversions and longer polymers. From the GPC traces, signals for tetramer, octamer, dodecamer, and hexadecamer can be clearly distinguished. The longer the oligomers become, the closer they move together, thus even longer oligomers merge together to a broad polymer band. Already the first oligomers are not baseline-separated, although they differ considerably by four repeat units. Optimization procedures could not improve the resolution; different eluents and column materials (normal and reversed phase) on a GPC and also on HPLC failed to resolve the oligomers of the mixture. Finally, the mixture was separated into fractions of enriched oligomers by preparative TLC, and the obtained fractions each further purified by a second preparative TLC run. With this procedure, fairly pure octamer **26a**, dodecamer **26b** and hexadecamer **26c** in addition to the tetramer **25** could be obtained (Table 1).

oligomer	repeat units	Mn (GPC)	PDI (GPC)	composition of isolated samples (UV230, UV280, RI)				
				% 4-mer	% 8-mer	% 12-mer	% 16-mer	% >16-mer
26a	8	6500	1.05	15, 20, 4	68, 63, 85	17, 17, 11	- , - , -	- , - , -
26b	12	8600	1.08	- , - , -	19, 21, 18	70, 60, 65	11, 19, 17	- , - , -
26c	16	9900	1.17	- , - , -	- , - , -	8, 9, -	84, 83, -	8, 7, -

Table 1: Results for the isolation of oligomers 26a-c out of reaction mixture. Purities determined by GPC; UV230, UV280, RI: different detectors of GPC set-up.

A microwave-assisted polymerization was also tried (50 W, 50-55 °C, 70 min) yielding a similar oligomer distribution as under standard reaction conditions, but in addition some non-aromatic low molecular weight material was obtained as revealed by GPC, presumably arising from decomposition reactions in the microwave.

2.6.5.2 Spectroscopic Characterization

The *ortho*-phenylene ethynylene oligomer series isolated from the polymerization of tetramer **25** was studied by optical spectroscopy to reveal potential conformational folding among this class of aromatic backbone structure. As the oligomers possess polar tetraglyme side chains, solvents of choice for studying solvophobic conformational changes and/or aggregation were chloroform as denaturing solvent and acetonitrile and acetonitrile-water mixtures for inducing folding/aggregation. The oligomers were studied separately as well as compared with each other to reveal chain length dependencies.

Figure 12, left, shows the absorbance and emission spectra for the *ortho*-phenylene ethynylene tetramer. When going from $CHCl_3$ to MeCN, the absorbance above 300 nm only slightly diminishes in accordance with a solvophobically driven conformational change from an extended planar conformation with a longer conjugation length absorbing at longer wavelengths to a non-planar compact conformation that avoids solvent contact and possibly resembles a helix. Changes in the emission spectra are more dramatic. While the fluorescence signal around 386 nm strongly diminishes, emission above 413 nm is much stronger in MeCN than in $CHCl_3$ arising from excimer formation[1] by stacking aromatic rings in either

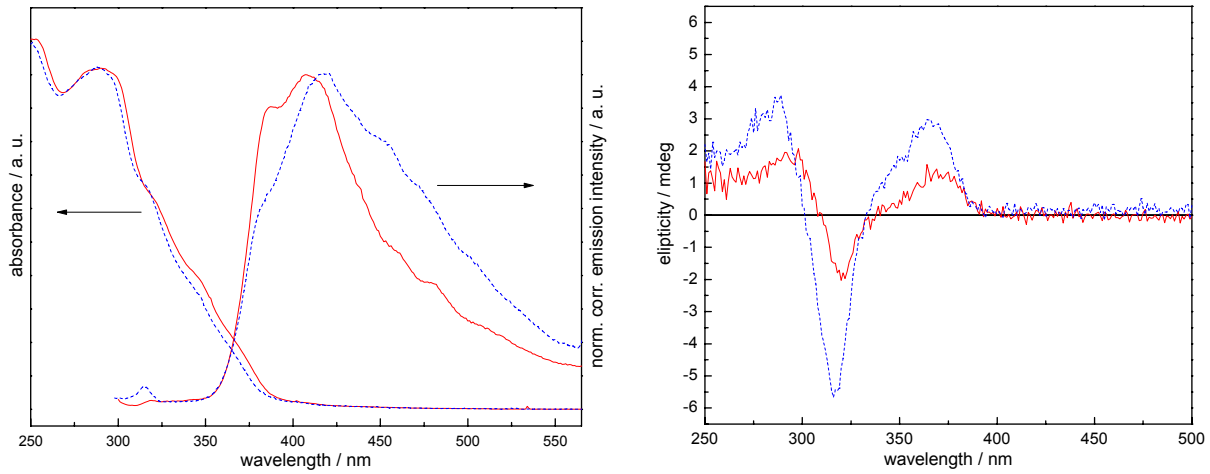

*Figure 12: Absorbance and emission spectra (left) and CD spectra (right) of tetramer **25** in chloroform (solid red) and acetonitrile (dashed blue) at same concentrations. Absorbance and CD spectra were recorded with an OD =1, emission with OD ≈ 0.1.*

[1] More correctly, a pseudo-excimer effect is observed, as the interacting aromatic moieties are pre-organized face-to-face due to folding.

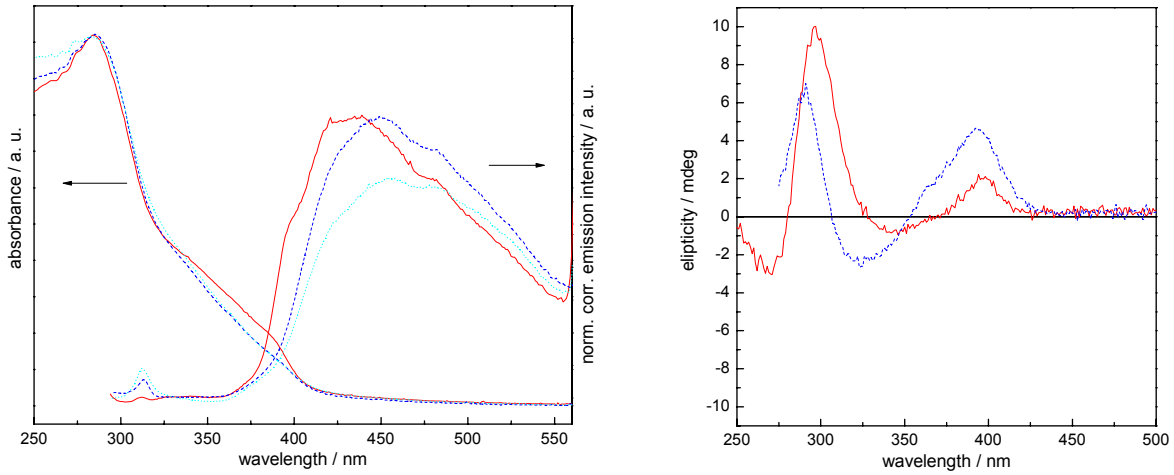

*Figure 13: Absorbance and emission spectra (left) and CD spectra (right) of octamer **26a** in chloroform (solid red), acetonitrile (dashed blue), and acetonitrile:water = 80:20 (dotted cyan) at same concentrations. Absorbance and CD spectra were recorded with an OD = 1, emission with OD ≈ 0.1.*

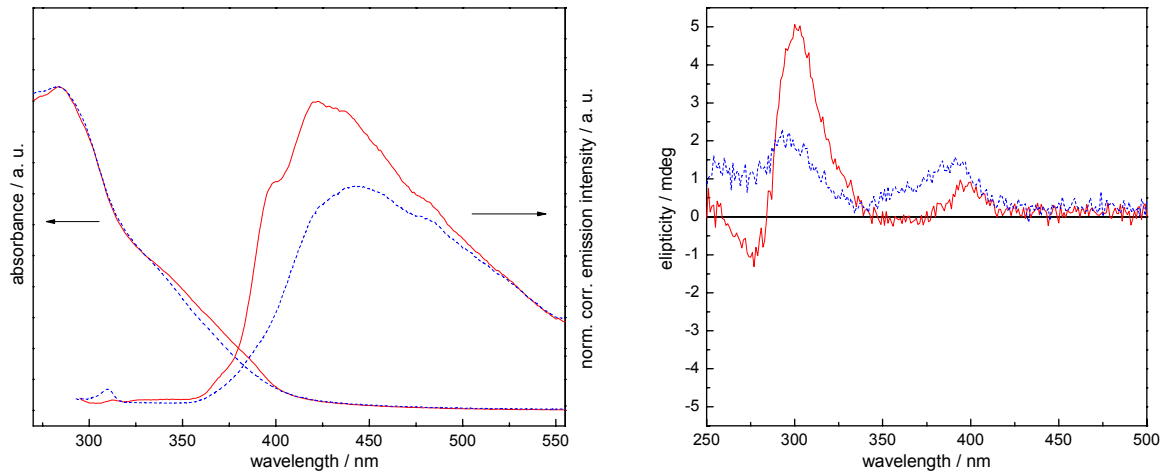

*Figure 14: Absorbance and emission spectra (left) and CD spectra (right) of dodecamer **26b** in chloroform (solid red) and acetonitrile (dashed blue) at same concentrations. Absorbance and CD spectra were recorded with an OD = 1, emission with OD ≈ 0.1.*

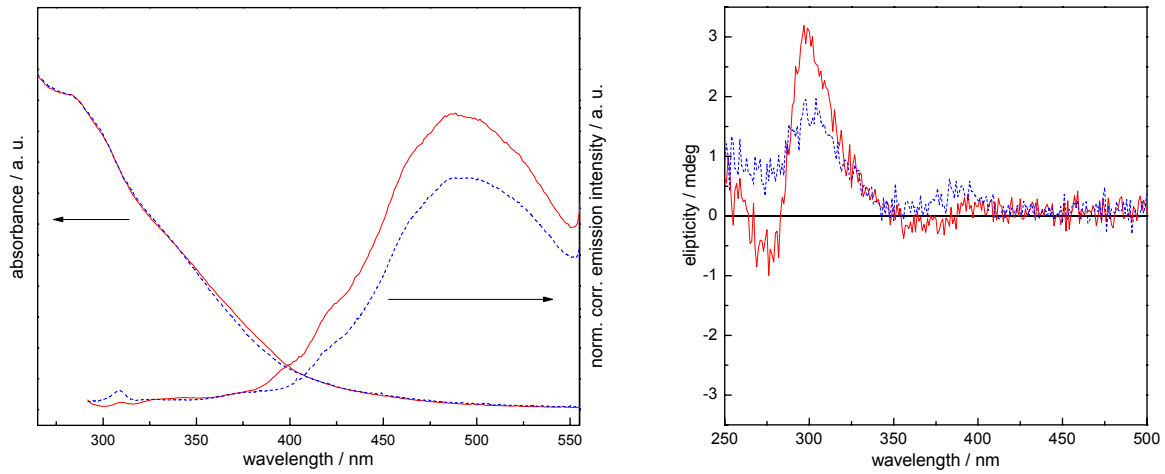

*Figure 15: Absorbance and emission spectra (left) and CD spectra (right) of hexadecamer **26c** in chloroform (solid red) and acetonitrile (dashed blue) at same concentrations. Absorbance and CD spectra were recorded with an OD = 1, emission with OD ≈ 0.1.*

intermolecular aggregates or intramolecular helical conformations. The corresponding CD spectra (Figure 12, right) disclose increasing optical activity by the tetramer in polar acetonitrile compared to chloroform. Three main signals can be identified; two positive signals around 300 nm and 375 nm, and a negative signal in-between around 325 nm. The exact electronic-structural source of the bands is not known, but the evaluation of the observed changes in absorbance and CD spectra support the following argumentation. The signals between 275 and 325 nm can be attributed to the aromatic units themselves (resembling more or less the absorbance of a single electron deficient phenyl molecule), while the region between 325 and 425 nm arises from π-conjugated and interacting units in extended zig-zag and helical conformation, respectively, becoming the main indicator of conformational changes. The decrease in absorbance intensity results from a lower absorbance coefficient ε(helix) of the helical conformation compared to ε(extended), due to distorted planarity and decreasing effective π-conjugation. The increasing optical activity in this region in polar solvents despite decreasing absorbance intensity further demonstrates the generation of a helical conformation.

The total optical activity further increases when going to the octamer and the two signals at longer wavelengths undergo a bathochromic shift of 25 nm each (Figure 13) in agreement with the increased absorbance interval. Optical activity is not only observed in acetonitrile, but in chloroform, too. When going from $CHCl_3$ to MeCN, the CD signal at 300 nm diminishes while at the same time, the signal at 400 nm increases. This effect is also observed among the longer oligomers (dodecamer in Figure 14, hexadecamer in Figure 15). For the tetramer, a limited concentration series was recorded and despite a low number of data points, only linear behavior was observed, ruling out at least the dominance of intermolecular aggregational changes on the observed optical effects.

In absorbance spectra of the octamer in chloroform, a strong absorption shoulder starts as additional feature at 325 nm and abruptly terminates around 400 nm. This absorption is correlated to an extended planar conformation possessing a longer electronic conjugation length with a narrower HOMO-LUMO gap as illustrated by the simple electron-in-a-box model. As less energy is needed for electronic excitations, absorption occurs at longer wavelengths. Also the fluorescence signal is red-shifted and in addition much broader compared to the emission of the tetramer as the number of electronic bands increases with conjugation length. In acetonitrile, the long-wavelength absorbance band decreases in accordance with the loss of structural planarity upon solvophobic folding. At the same time, the fluorescence signal around 400 nm diminishes and emission above 450 nm increases due

to induced excimer emission upon compacting the molecular structure. Addition of up to 20 % water to acetonitrile solutions did not notably increase the effects observed when going from chloroform to acetonitrile with respect to absorbance or circular dichroism spectra, only the fluorescence intensity diminishes without any change of band shape.

The effects in absorbance, emission, and circular dichroism are less pronounced with the longer oligomers. The spectra's shape and position of the dodecamer resemble more or less those of the octamer: the shoulder in the absorbance spectrum in chloroform is less developed and the absolute signal intensities in the CD spectra decreased and these trends continue for the hexadecamer. Starting with the dodecamer, the fluorescence intensity in acetonitrile is lower than in chloroform, possibly due to a new aggregation motif in solution that quenches fluorescence and lowers concentration of optically active conformations. The fluorescence spectra of the hexadecamer in both solvents are in addition red-shifted and are now centered around 500 nm. Figure 16 shows an overlay of CD spectra for the oligomer series in chloroform and acetonitrile with signal intensities corrected to number of repeating units in solution. The strongest signals are observed for the octamer (magenta, dashed), whereas the dodecamer (violet, short dashed) displays medium intensities and the hexadecamer (blue, dotted) the lowest in terms of $\Delta\varepsilon$. Apparently, with the octamer an optimum chain length is reached for inducing maximal absolute optical activity as well as maximal changes. If we attribute this optical activity – and the results of the other complementary optical spectroscopy methods – to helical folding, then for longer backbones folding into an ordered compact helical structure might be more difficult for steric or thermodynamic reasons, or another conformational alternative or aggregation might be favored at the expense of the intramolecular helical structure.

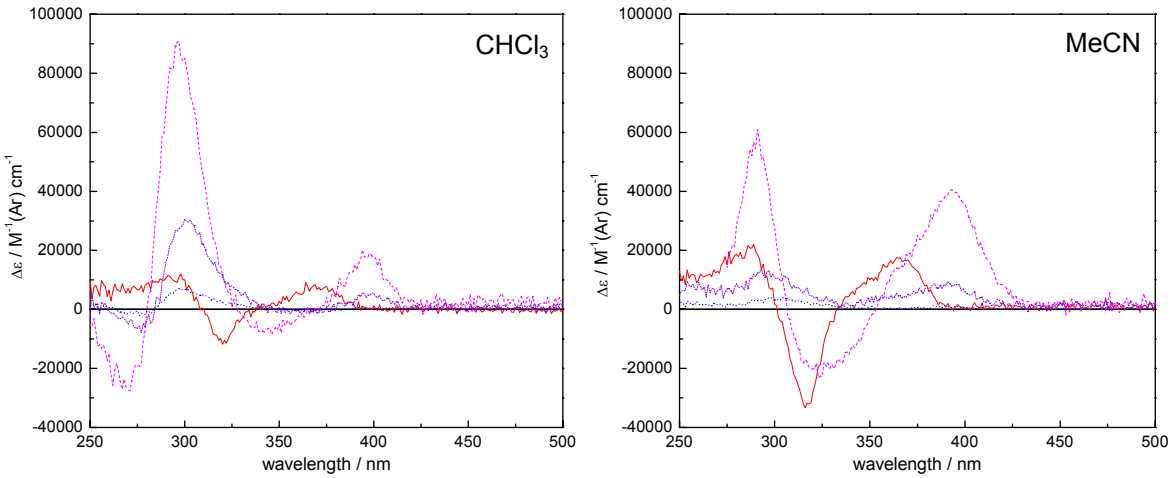

Figure 16: Overlay of CD spectra of tetramer (solid red), octamer (dashed magenta), dodecamer (short dashed violet), and hexadecamer (dotted blue) in chloroform (left) and acetonitrile (right). Traces were recorded at OD = 1 and corrected with respect to concentration of aromatic units per solvent volume.

In order to study thermodynamics of the folding process, solvent titration series of the octamer in solvent gradients from acetonitrile-water mixtures to neat chloroform were recorded. Figure 17 illustrates the results for the different optical spectroscopic methods. All calculated signal intensity ratios show non-linear behavior implying a cooperative conformational change of the oligomer's backbone. As the transition represents to a shallow slope, the involved thermodynamic driving force for folding and unfolding is small. As the helical folding of *ortho*-phenylene ethynylenes involves strong phenyl distortions from planarity, the helix-stabilizing aromatic π-π-interactions might be small. Folding saturation is reached in polar acetonitrile as monitored by absorbance, emission, and CD spectroscopy, and the addition of water does hardly push the observed effects further. When approaching the other extreme of neat chloroform solutions, a decrease of the slope is observed in absorbance and emission, but no horizontal plateau is reached, indicating the presence of random disordered conformations of the backbone more than planar fully extended conformations. A fully sigmoidal progression with horizontal baselines at both titration extremes needed for calculating helix stabilization energies was not obtained.

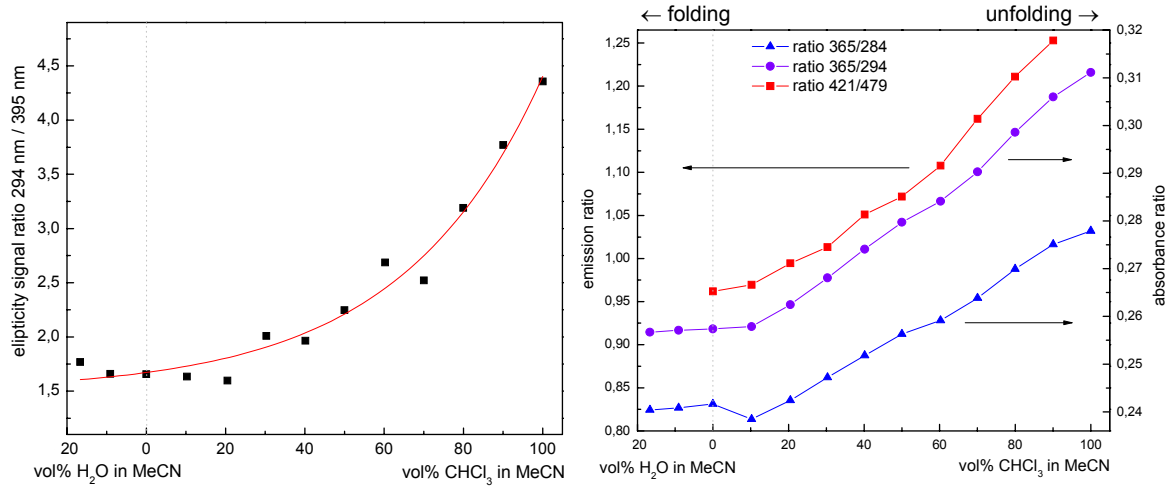

Figure 17: Titration series of octamer from 20 % water in acetonitrile via neat acetonitrile to chloroform. Left: ratio of elipticity signals 294 nm / 395 nm, right: emission ratio 421 nm / 479 nm (■) and absorbance ratios 365 nm / 294 nm (●) and 365 nm / 284 nm(▲).

Figure 18 displays the spectra of the oligomeric *ortho*-phenylene ethynylene mixture before isolation of the individual oligomers. The comparison of the normalized absorbance spectra recorded in different solvents accentuates the strong additional feature between 325 nm and 400 nm, already identified in the octamer spectra and attributed to an extended backbone conformation. Surprisingly, emission is much stronger in polar acetonitrile than in chloroform. The CD spectra correlate more or less with the spectra of the isolated oligomers, although here the signal at 400 nm is clearly less intense than expected. Again, the signals below 350 nm are much stronger in chloroform than in acetonitrile.

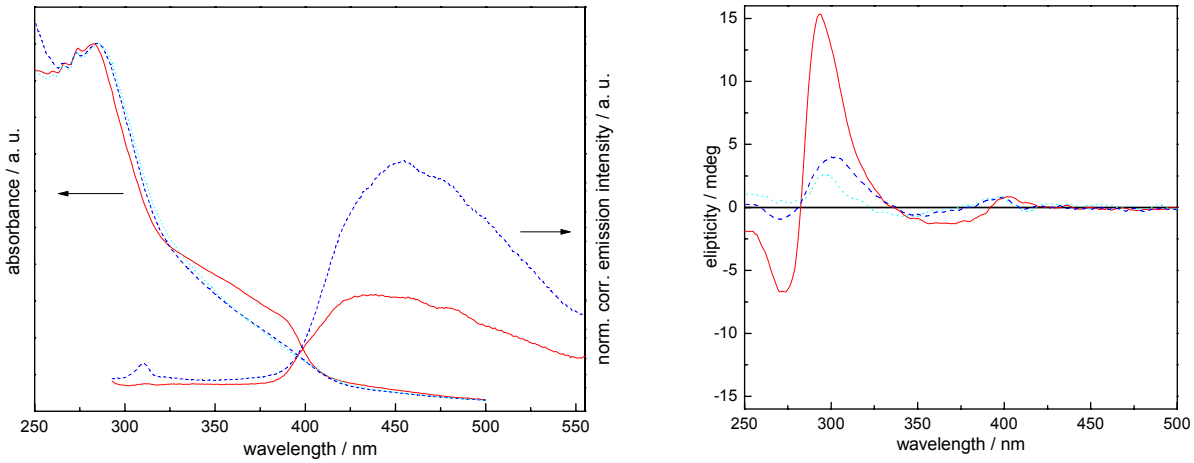

Figure 18: Absorbance and emission spectra (left) and CD spectra (right) of oligomeric mixture in chloroform (solid red), acetonitrile (dashed blue), and acetonitrile-water mixtures (dotted cyan). Absorbance and CD were recorded at OD = 1 and emission at OD = 0.1.

2.6.6 Soluble Phase Synthesis

2.6.6.1 Introduction

Back in 1963, Merrifield revolutionized the field of peptide chemistry by introducing the solid phase synthesis methodology.[36] Here, the starting material is covalently anchored on a solid support – often a cross-linked polymer – and all the chemical transformations leading to the target molecule are performed with the intermediates staying covalently attached to the support. In the final step the desired product is then cleaved and separated from the support. In a similar manner works the soluble support strategy,[49] often also wrongly called liquid support strategy. Prerequisite for a suitable support is a polymer well soluble under the indented reaction conditions. Polystyrenes, poly(vinyl alcohol)s, and poly(ethylene glycol)s are reported on as standard soluble supports and were used to either synthesize small organic molecules, biomolecular sequences (peptides, oligonucleotides, or oligosaccharides) or used as scaffolds for recoverable catalysts and reagents[50] and for polymer therapeutics.[51]

The number of anchoring sites should be restricted to one or two functional groups per polymer strand; otherwise, discrimination in their reactivity is often observed. The ideal polymer length resembles a compromise between dominating the solubility properties (the larger the target structure the longer the polymer chain) and loading capabilities (shorter chains increase loading in terms of grams of product per grams of support) and has to be chosen in accordance to the synthetic target.

The key advantage of a soluble support over a solid phase is to allow for homogeneous reaction conditions and thus prevent common problems including nonlinear kinetics, bad and unequal access to reaction sites, and time-consuming optimization of standard reaction protocols to the solid phase. Once the reaction terminated, the soluble support can be precipitated and filtered off leaving unreacted material and impurities in solution.

Biomolecules are the general target when applying solid or soluble support methodologies for generating oligomer sequences, and there are only two examples for phenylene ethynylenes synthesized on a solid support: Anderson[7] generated a series of differently linked pentamers on polystyrene applying a “tea bag” procedure to carry out several different couplings simultaneously in a parallel fashion while Moore and coworkers constructed *m*PE-oligomers up to the hexamer anchored via a triazene moiety to a solid polystyrene support.[52]

In this work, the synthesis of *ortho*-connected phenylene ethynylenes on a soluble support was addressed. Poly(ethylene glycol) (PEG) was utilized as support, as an adequate polymer length can be chosen from a wide range of commercially available PEGs. Its good solubility

in many organic solvents, its chemical robustness, and the lack of interfering aromatic units for NMR monitoring are additional arguments. The terminal hydroxyl groups allow the anchoring via an ester moiety, which is convenient for formation, stability during oligomer synthesis, and smoothness of final cleavage.

As the Sonogashira coupling is based on two orthogonal functional groups, two synthetic routes for a stepwise construction of the oligomer sequence are accessible, either head to tail or tail to head. Working with iodo-terminated anchored species (Figure 19, top) intrinsically prevents the incorporation of diine defects, as such diines can only be formed by dimerizing monomers in solution and are thus subsequently washed away. On the other hand, having the acetylene anchored on the support (Figure 19, bottom) facilitates the (complete) activation prior to the coupling step.

2.6.6.2 Synthesis of Phenylene Ethynylenes on PEG-Support

The synthesis of conjugated *ortho*-phenylene ethynylene oligomers via soluble-phase based chemistry started with the anchoring of 4-iodo-benzoic acid chloride **28** – generated from the corresponding acid **27** with oxalyl chloride – to the bishydroxyl-terminated poly(ethylene glycol) (Mn = 8000 g/mol; see Scheme 11). After all steps, purification followed a sequence of precipitating the polymer in diethyl ether from a concentrated CH_2Cl_2 solution, washing or recrystalizing in ice-cold ethanol, and finally precipitating again in diethyl ether from a

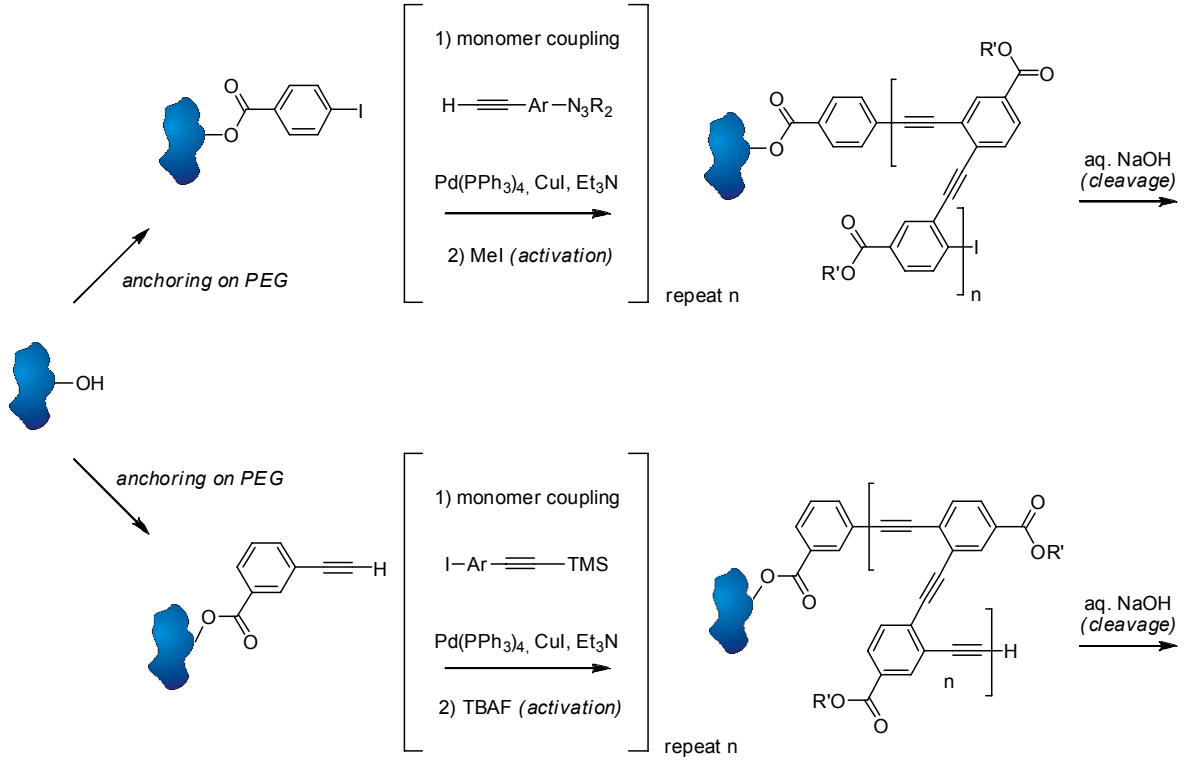

Figure 19: Synthetic approach to phenylene ethynylene oligomers via stepwise coupling on a soluble support.

CH_2Cl_2 solution and extended drying in vacuo. With this procedure, non-polar as well as polar material is removed. The third precipitation step is required to remove major amounts of encapsulated and non-volatile polar solvents. Due to the intrinsic low loading capacity of soluble supports and the envisioned long synthetic route, all reactions were ran on a multigram scale up to 35 grams, further aggravating a rapid progress. To prove complete coverage of the support adduct **29** was treated with a large excess of acetic anhydride, but no acylation could be observed by NMR, thus assuming complete anchoring.

Then a large excess of phenyl acetylene **13** was coupled by Sonogashira-reaction to the PEG-derivative **29** (Scheme 11, top), generating an anchored PE-dimer. Subsequent saponification allowed isolation of the bisacid derivative **31** of the PE-dimer in moderate yield and purity, resembling the coupling product of both complementary capper building blocks presented in the preceding chapter.

Starting from the same PEG-anchor system **29**, orthogonal functionalized monoactivated *o*PE-monomer **6** was coupled in large excess to the soluble support. Although working under homogeneous conditions, all Sonogashira reactions as well as activation steps had to be run for prolonged times and elevated temperatures to achieve complete consumption of starting materials, e. g. the triazene-iodo exchange on **32** ran for two days instead of several hours until pyrolidine protons disappeared from ^{1}H-NMR spectra. Capping of the activated PE dimer with excess of **13** finally gave the desired *o*PE bound to the PEG-support.

Due to the poor triazene-iodo-exchange on the PEG-bound aromatic units, the synthetic route to PE-oligomers was addressed in an alternative approach, using the opposing functional groups on support and reactants than before. By having the TMS-acetylene functionality on the PEG-based soluble support, the iterative oligomer build-up is now based on the reliable acetylene deprotection at the end of the growing oligomer followed by addition of an appropriated monomer carrying the iodo functionality.

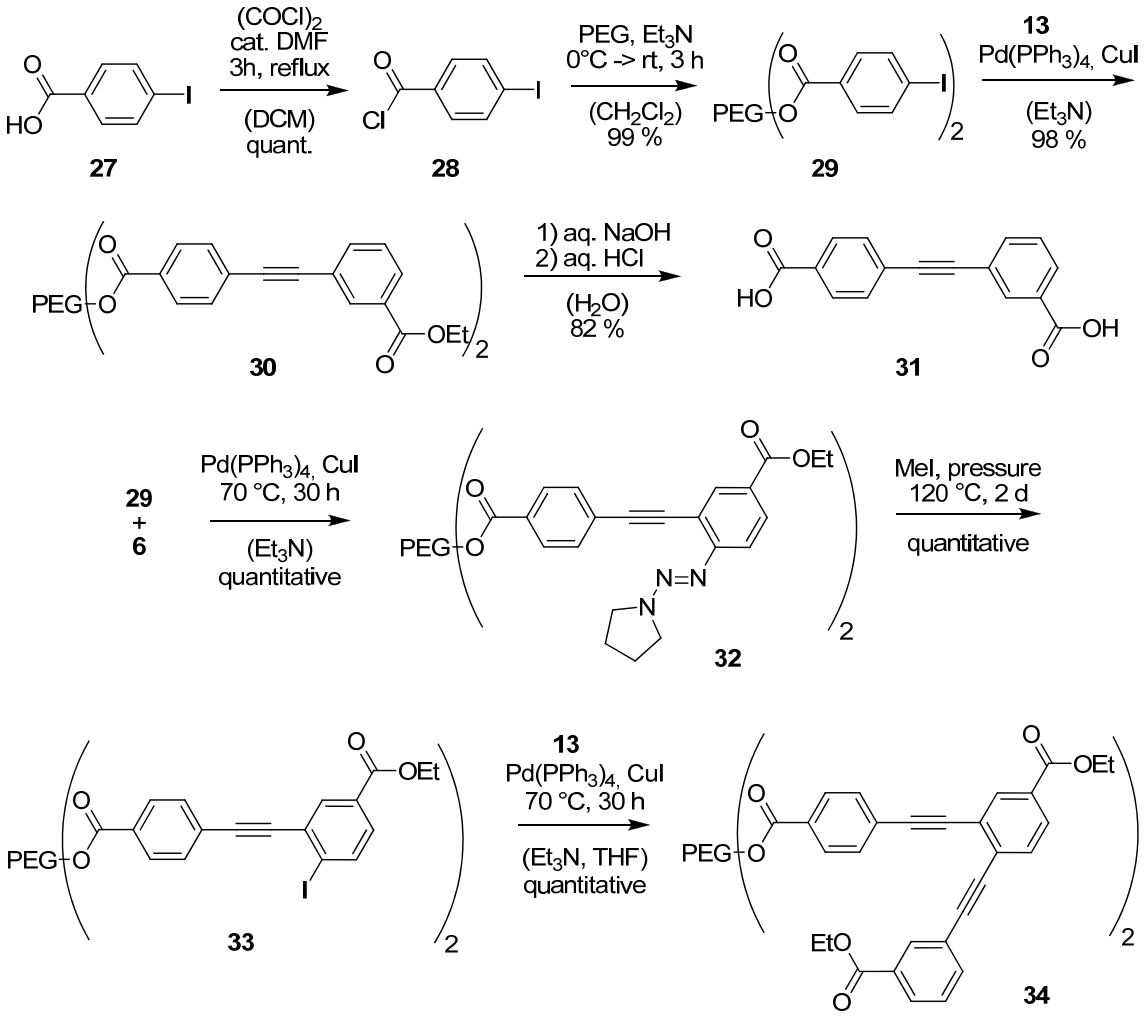

Scheme 11: Top: anchoring of aryl iodide on bishydroxyl terminated poly(ethylene glycol) via ester moiety and subsequent generation and cleavage of phenylene ethynylene dimer; bottom: synthesis of phenylene ethynylene trimer on soluble support.

Activation of 3-bromo-benzoic acid with oxalyl chloride to the corresponding acid chloride allowed its coupling to bishydroxy-terminated PEG under DMAP catalysis yielding PEG-support **36** with anchor moieties on its both ends (Scheme 12), followed by TMS-acetylene coupling to the anchors by standard Sonogashira. TMS-deprotection of **37** had to be performed at relatively harsh conditions: only refluxing for three hours in threefold excess of fluorides yielded the desilylated intermediate as confirmed by ^{1}H-NMR. Sonogashira coupling with threefold excess of *ortho*-monomer **5** afforded the TMS-protected PE dimer bound on PEG-support (compound **38**); again, prolonged reaction times were needed to achieve complete coupling as monitored by NMR and the bulk material acquired a creamy consistency lengthening purification procedures. For the next coupling cycle, **38** was desilylated with TBAF, purified, and subsequently coupled with an excess of ethyl *para*-bromobenzoate to render the PEG-bound PE trimer **39**, being identical to **34** but bound to the support with its opposing end.

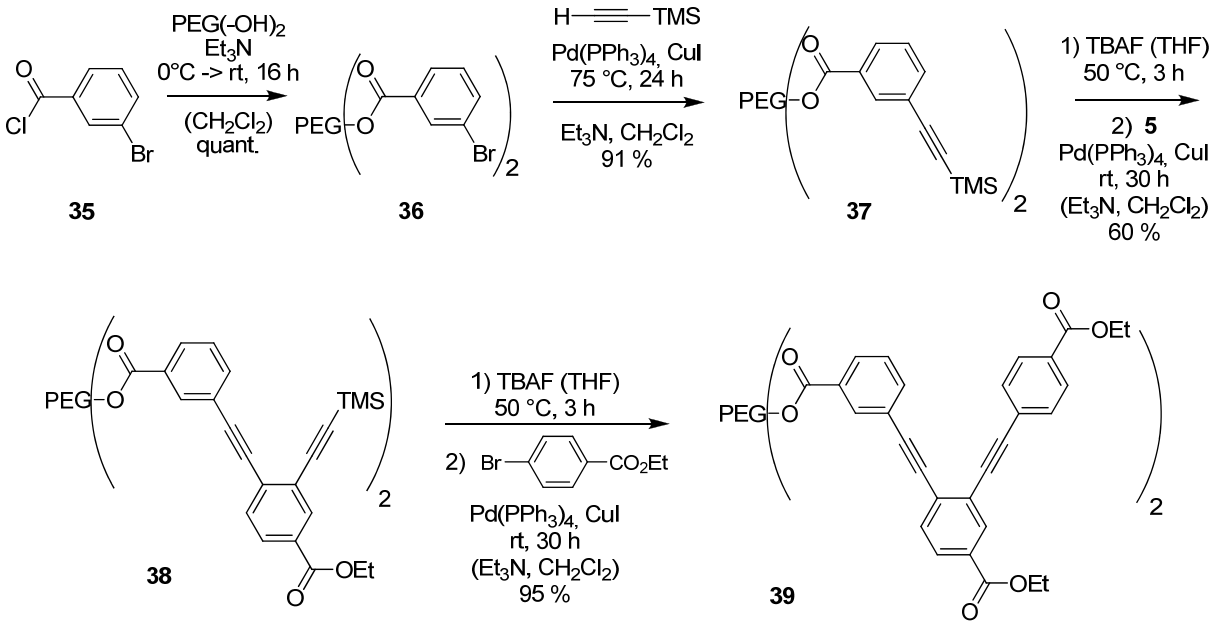

Scheme 12: Alternative route to PEG-supported ortho-phenylene ethynylene trimer based on an acetylene bound strategy.

The synthesis of *ortho*-phenylene ethynylenes was not pursued further for several reasons. The initially easy purification by precipitation turned out to be less satisfying than expected. Washing and filtering of the large amounts of precipitated PEG due to the low loading level was time consuming as the polymer encapsulated undesired material upon precipitation and clogged filters; drying of the obtained solid took long periods of time and thus traceless removal of solvents and impurities was hardly possible. With growing PE on the PEG, consistency of material became creamy further aggravating filtration steps. The loading capacity of the used PEG was limited, and monitoring of the reaction progress was not possible by TLC and hard with other techniques such as ^{1}H-NMR. Key activation steps were not satisfying, as triazene-iodo exchange incomplete, and full desilylation required longer reaction times at elevated temperatures. The difficult *ortho*-Sonogashira coupling was further aggravated by the steric bulk of the polymer and large excesses of material had to be used, taking into account also the limited reaction monitoring possibility. Finally, this usage of excesses of precious material – i.e. monomers and cappers synthesized by several-step-procedures with moderate overall-yields – uncovered this synthetic approach as a wasteful one in terms of material and the potential re-isolation of excess monomers would have turned the whole procedure absurd.

However, the accumulated expertise with polyethers and “block copolymers” was utilized and expanded as described in Chapter 3, where “real” block copolymers on the basis of poly(propylene oxide) and poly(phenylene ethynylene) are discussed.

2.7 ortho-alternating-para-Phenylene Ethynylene Based Polymers

2.7.1 Approach

The retrosynthetic analysis of target monomer **40** leaded to three building blocks, first a 1-(TMS-ethynyl)-4-triazenylbenzene **41** as the *para*-component, second, an *ortho*-dibromophthalic acid derivative **43** as central core, and third, a suitable amine **42** as branched chiral side chain (Figure 20), derived conveniently from an enantiopure natural amino acid.

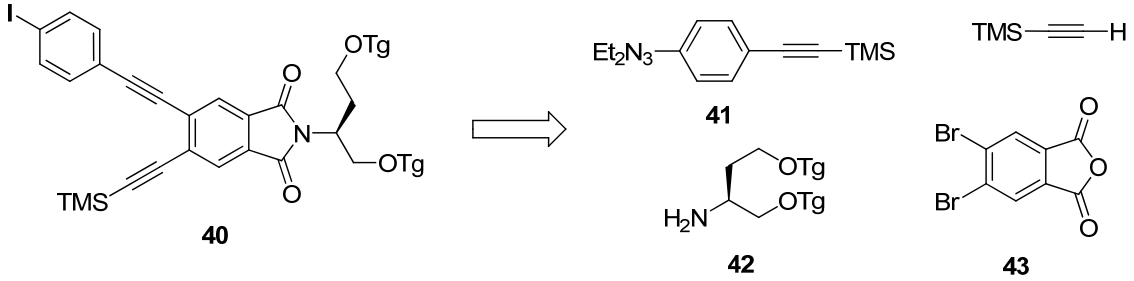

Figure 20: Retrosynthetic analysis of ortho-alternating-para-phenylene ethynylene monomer.

2.7.2 Aromatic Cores – *para*-Building Block

The synthesis of the *para*-building block **41** is straightforward and resembles the monomer synthesis. Starting from *para*-iodoaniline **44**, the amino group is transformed via the diazonium salt into the triazene in excellent yields (Scheme 13). Sonogashira coupling of an excess of TMSA to the iodo functionality proceeded smoothly due to favorable electron deficiency on the arene and choice of halogen, still, purification by column chromatography was required. Desilylations by either carbonates or fluorides proceeded in quantitative yields.

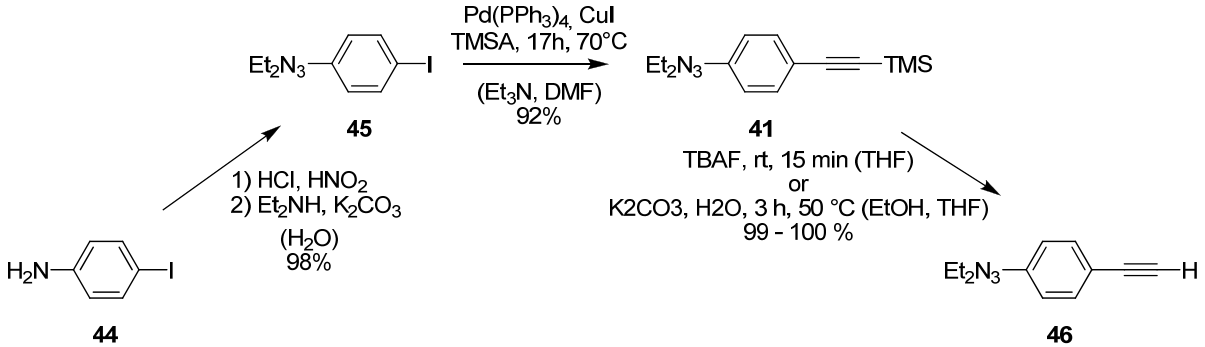

Scheme 13: Synthesis of para-building block 1-ethynyl-4-(diethyltriazenyl)benzene.

2.7.3 Aromatic Cores – *ortho*-Building Block

The route to the difunctional *ortho*-building block based on *ortho*-xylene (Figure x). The latter was bisbrominated as described in the literature[53] and purified by recrystallization. Simultaneous and complete oxidation of both methyl groups of **48** to carboxylic acid functionalities was achieved with permanganate as the oxidant. Recrystallization from water

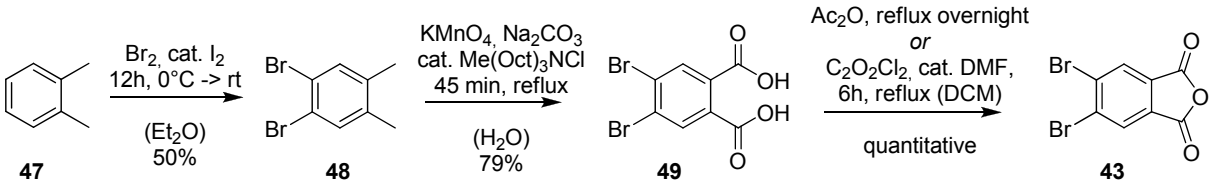

Scheme 14: Synthesis of dibromophthalic anhydride core building block.

gave the desired phthalic acid **49** with relatively high amounts of incorporated water molecules that were azeotropically removed by concentrating corresponding toluene suspensions se veral times. In the following step, intramolecular ring closing to the corresponding anhydride **43** was performed with either acetic anhydride[54] or oxalyl chloride.

2.7.4 Model Monomer

Synthesis of a model *ortho-para*-monomer and its polymerization demonstrated the feasibility of the proposed synthetic route to such class of *ortho*-alternating-*para*-phenylene ethynylene monomers (Scheme 15). Previously synthesized 4,5-dibromophthalic anhydride **43** was reacted with *n*-butylamine to give the corresponding phthalimide **50** in excellent yields. While condensation of aromatic amines with phthalic anhydride run smoothly without any additives, N-alkyl imides are more difficult to prepare and a protocol including the use of $ZnBr_2$ and HMDS was followed,[55] based on the extensive Silicon work of Vorbrüggen.[56] The mixed amide-acid formed in the first step, is activated by the Lewis acid $ZnBr_2$ coordinating to the carbonyl oxygen of the free acid group while HMDS generates intermediate species containing silanol leaving groups thus facilitating intramolecular cyclization. Sonogashira condensation of phthalimide **50** with one equivalent of freshly prepared 1-ethynyl-4-(diethyltriazenyl)benzene **46** gave a mixture of 50 % monocoupled and 25 % biscoupled products, among others. After separation, the monocoupled adduct **51** was condensed with an excess of TMSA again via Sonogashira reaction to give the orthogonally

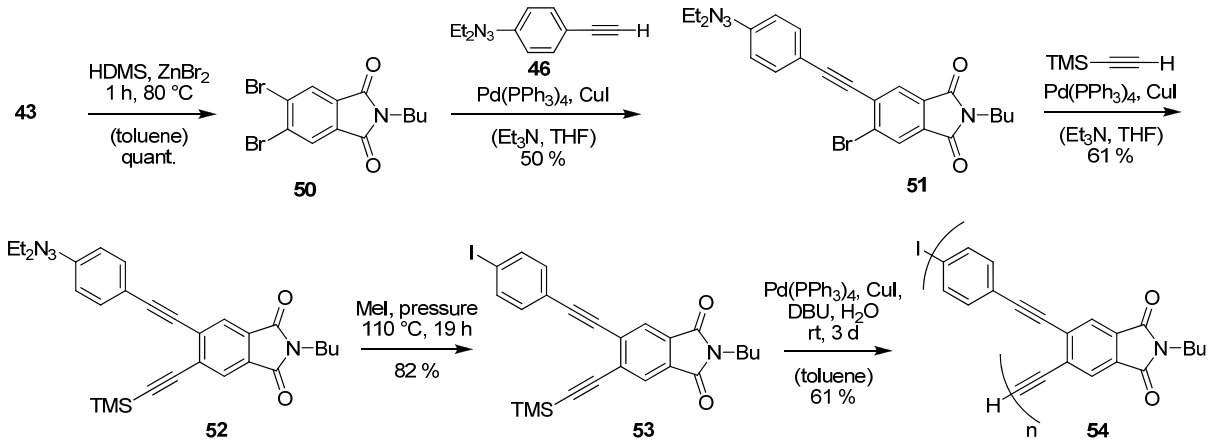

Scheme 15: Synthesis of ortho-alternating-para-phenylene ethynylene model monomer and its polymerization.

protected *ortho-para*-monomer **52**. After subsequent triazene-iodo exchange, model monomer **53** could successfully be polymerized to give fractions with oligomers up to 14 r. u. length as shown by GPC. In view of this promising result, the focus changed to the design of a more demanding side chain.

2.7.5 Synthesis of Chiral Branched Polar Side Chain

Aspartic acid **55** was chosen as starting material to generate a branched chiral side chain. The utilization of this natural amino acid carrying an intrinsic chiral center in high enantiopureness spared the stereoselective/asymmetric synthesis of suitable starting material or separation of racemic adducts. The direct twofold reduction of the amino acid to the bisalcohol **57** failed probably due to the general low solubility of the acid in organic (aprotic) solvents. Instead, the acid could effortlessly be esterified twice to the dibutyl aspartate **56**, followed by $LiAlH_4$ reduction to the aminodiol **57** (Scheme 16). Due to its extreme polarity, the crude product had to be isolated from the aluminum adducts by prolonged Soxhlet extraction. Purification was achieved by Kugelrohr distillation under vacuum.

Protection of the amino group turned out to be more difficult than expected due to its low solubility and competing functional groups. Condensation with phthalic anhydride without[57] or with applying the $ZnBr_2$/HMDS protocol[55] (Scheme 16, bottom, left) rendered a complex mixture of the desired imide **60** and bisesters, bisamides, and esteramides. Transformation of aspartinol to the corresponding imine **59** (Scheme 16, bottom, center) by condensation with benzaldehyde failed, neither via azeotropic removal of water[58] nor with homogeneous drying agents like orthoformates.[59] Major products were all kind of (mixed) acetales.

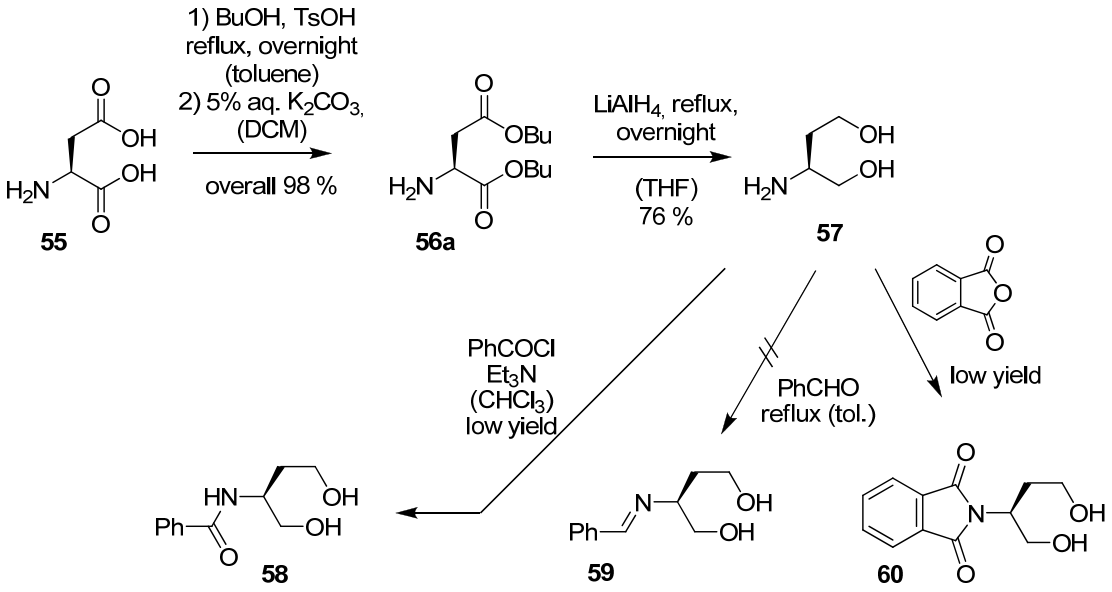

Scheme 16: First attempts to access N-protected aminodiol derivatives of aspartic acid.

2.7.6 Benzoyl Route

Following an alternative route to the protected aspartinol derivate **65**, aspartic acid **55** was subsequently esterified and N-protected as amide with benzoic acid chloride. Reduction of the dibutyl ester **64** to the corresponding diol was first tried with $NaBH_4$, but even refluxing did not initiate any conversion, opposed to some literature sources.[60] With $LiBH_4$, complete reduction was accomplished under mild conditions leaving the amide functionality intact and yielding crystalline N-benzoyl aspartinol in excellent yield and purity, while reduction with an equimolar combination of LiCl and $NaBH_4$ needed 24 hours refluxing for completion, possibly due to the low solubility of LiCl in THF. In parallel, triethylene glycol monomethyl ether **61** was activated by transforming the hydroxyl group into a more reactive tosyl or bromide function (Scheme 17, top). Tosylation worked with ease in excellent yields and purity, and gratifyingly, ether coupling and subsequent purification worked better with tosylates than with the corresponding bromides. Neat sodium hydride as well as the corresponding suspension in mineral oil was used for alcohol deprotonation leading to similar results, although the latter is more unproblematic concerning handling. Bisetherifications with triglyme bromide and triglyme tosylate, respectively, were run in parallel. In both procedures, TBAI and 15-Crown-5 were added as transfer catalysts to improve typical incomplete conversions und moderate yields. For the first time in this synthetic route, purification by

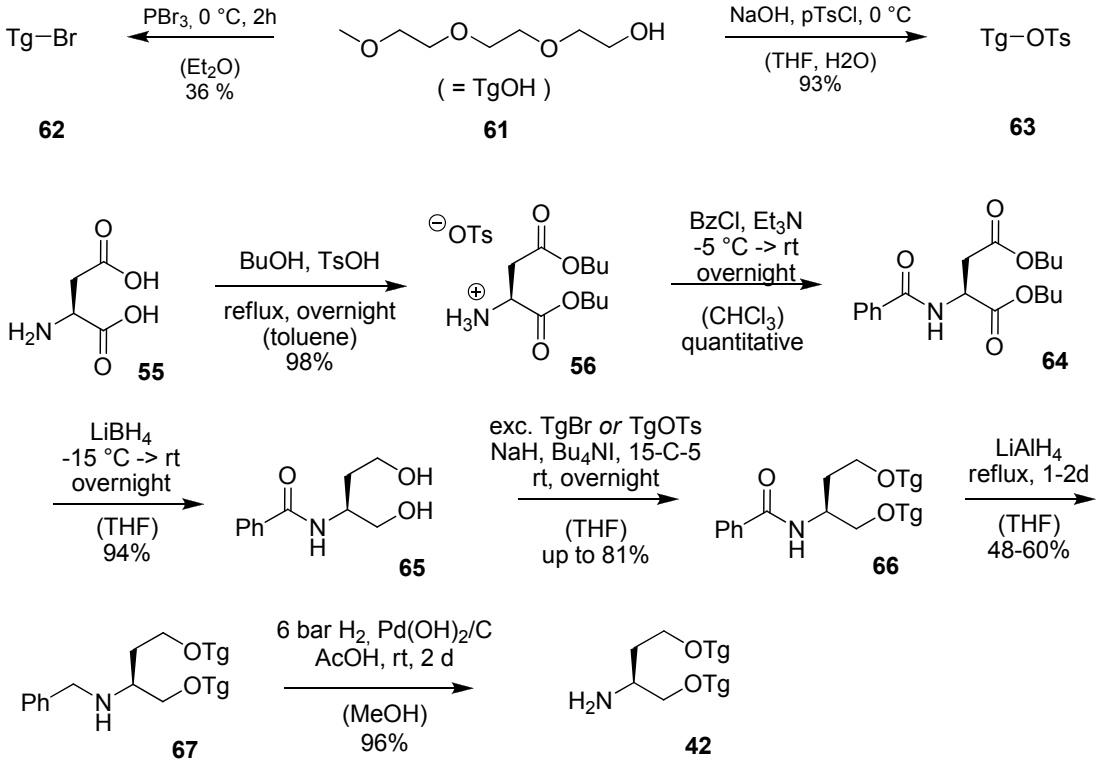

Scheme 17: Activation of triethylene glycol monomethyl ether (top) and successful synthetic route to polar, branched, and chiral side chain based on aspartic acid (bottom).

column chromatography was needed to remove monocoupled adduct, TBAI, and 15-Crown-5, and excess triglyme starting material, all displaying similar polarities and in part poor visibility on TLC.

The direct cleavage of the benzoyl moiety of **66**, either under harsh basic or acidic conditions failed. When refluxing the amide in concentrated sodium hydroxide solutions, only starting material could be isolated. On the other hand, refluxing the amide in concentrated aqueous hydrochloride did lead to the cleavage of the benzoyl group, but at the same time the triglyme chains were severely fragmented; as a result, no intact desired amine could be isolated.

The longer, but seemingly easier pathway to the free amine **42** proceeds via the benzyl intermediate **67**. Surprisingly, reduction of the amide with $LiAlH_4$ under standard conditions could not be driven to completion. Instead, starting material had to separated by column chromatography from the smearing product. Although the cleavage of N-benzyl groups by hydrogenolysis catalyzed by Pd/C is described in the literature,[61] it failed under standard conditions and only starting material was reisolated. The more potent Pearlman's catalyst, $Pd(OH)_2/C$, is often reported as the better catalyst for N-benzyl cleavages under mild conditions.[62] Still, elevated hydrogen pressures up to 6 bar, equivalent amounts of acetic acid, and prolonged reaction times had to be applied in addition to Pearlman's catalyst to accomplish the necessary complete conversion to the desired free amine **42**, as mixtures were inseparable.

2.7.7 Anthracenoyl Route

The idea of using anthracene instead of phenyl as a protecting group and UV-tag seamed very promising. Aspartic acid was esterified as before and the corresponding ammonium salt was condensed with freshly prepared anthracene-9-carbonyl chloride to the desired amide **69** (Scheme 18). Controlled reduction of both ester groups with $LiBH_4$ gave the corresponding N-protected aspartinol **70** in moderate yields. At this point, an additional purification by column chromatography was needed in contrast to the benzoyl route; the very polar aspartinol fragment dictated the overall behavior on TLC/column and lead to noticeable smearing. Bisether formation by coupling triglyme tosylate **63** to the aspartinol derivative **70** in the presence of TBAI and 15-Crown-5 gave the desired product in only modest yields opposed to the coupling in the benzoyl route. In addition, the purification of the bistriglyme product **71** was not easier than with the benzoyl derivative; it was hoped that the anthracene would induce more hydrophobicity and thus increase discrimination from byproducts.

The painful surprise turned up with the LAH-reduction of the amide. Using standard reducing conditions, not only the amide was reduced but also the central anthracene ring, sometimes reported in literature[63] (Scheme 18). Only very few publications could be found where anthracene carbonyl compounds were reduced, and this was always achieved with boranes. The work-up of borane reductions consists of refluxing in concentrated mineral acids,[64] but this was shown to fragmentize the triglyme chains while acidic treatment at room temperature or short heating was not sufficient to saponify the intermediate borates. In analogy, the attempted direct cleavage of the anthracene carbonyl moiety in concentrated acids leaded to fragmentation even when refluxing for short periods of time. A reoxidation of the dihydroanthracenyl moiety followed by hydrogenolytic cleavage of the anthracenylmethyl group was not attempted.

2.7.8 Assembly of Building Blocks to Final *ortho*-alternating-*para*-Phenylene Ethynylene Monomer and Its Polymerization

The synthetic approach to the *ortho*-alternating-*para*-PE monomer **40** carrying the chiral branched polar side chain resembled the route followed to access the model monomer **53**. Once the side chain amine **42** was obtained, it was condensed with dibromophthalic anhydride **43** to the corresponding imide following the proven $ZnBr_2$/HMDS protocol[55] (Scheme 19). Sonogashira coupling with freshly deprotected *para*-building block **46** rendered after extended purification the monocoupled adduct **74**. Yields were surprisingly good, probably due to sterically hindered biscoupling to the phthalimide core. The usage of a large excess of TMSA in the next step gave the orthogonally protected monomer **75** in quantitative yield, but

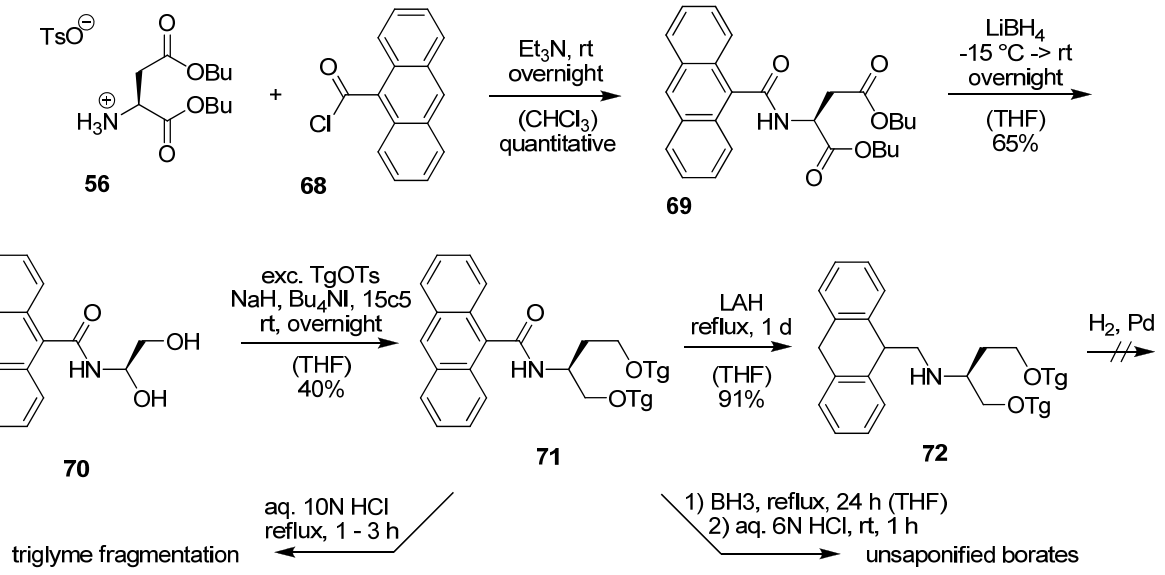

Scheme 18: Alternative synthetic route to N-protected 1,4-bis(triglyme) aspartinol using anthracene acid chloride and failed deprotection.

still requiring further purification. Triazene-iodo exchange was carried out in neat methyl iodide at elevated temperatures and pressure providing the final polymerizable monomer **40** in satisfying yield. As in most steps of this synthetic route, the desired product had to be purified by extended column chromatography as the identical side chain among the different adducts governed the polarity. HPLC on three different chiral columns did not reveal racemization of the chiral center of the monomer. Thus, retention of enantiomeric excess of the starting amino acid throughout the synthetic route is assumed despite the lack of a racemic sample for direct comparisons.

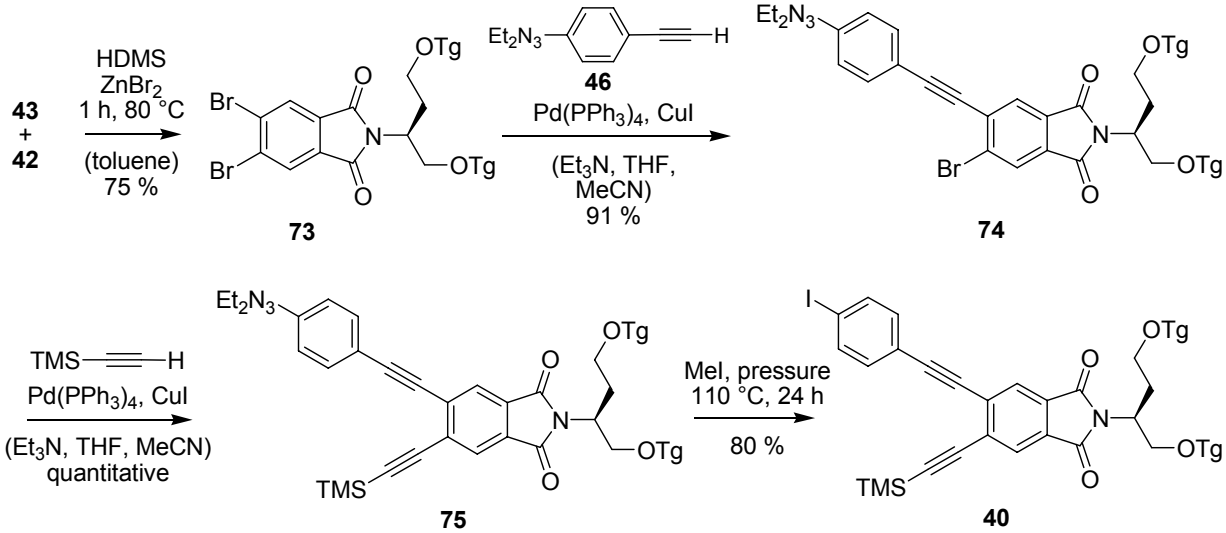

Scheme 19: Linear synthetic route to the final ortho-alternating-para-phenylene ethynylene monomer carrying a chiral branched polar side chain; Tg = triethylene glycol monomethyl ether.

Finally, the monomer **40** was polymerized under Sonogashira conditions applying the *in-situ* desilylation protocol[19] (Scheme 20). Stirring at room temperature for three days afforded an oligomeric mixture with n = 2 - 10 according to GPC, resembling approximately a tetra- to decamer with 4 to 20 aromatic units.

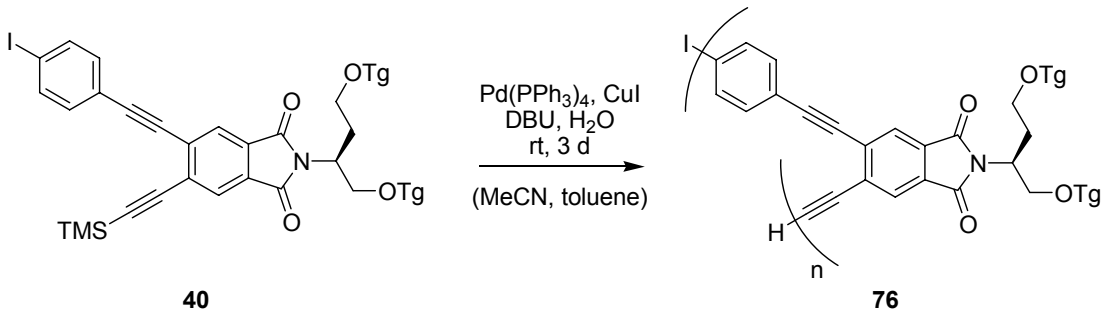

Scheme 20: Polymerization of ortho-alternating-para-phenylene ethynylene monomer carrying a polar branched chiral side chain.

2.7.9 Initial Spectroscopic Characterization of ortho-Alternating-para-Phenylene Ethynylene Polymer

The obtained oligomeric *ortho*-alternating-*para*-phenylene ethynylene mixture was analyzed by absorbance, fluorescence and CD spectroscopy. Figure 20 shows the corresponding spectra in different solvents. The bimodal absorbance spectra display two main features, a signal at 300 nm and at 350 nm. In analogy to spectra of *o*PE systems, the band at lower wavelength is associated with the absorbance of single repeating units and stays constant upon solvent changes. Contrary, the absorbance above 325 nm decreases in polar acetonitrile and might be interpreted as a depopulation of planar extended conformational states due to folding and decline of effective conjugation length. Concerning fluorescence, the solvent influence on the spectra is surprisingly moderate. The emission is bathochromically shifted compared to *o*PEs as expected for an enlarged effective conjugation length and the intensity at lower wavelengths decreases in acetonitrile in accordance with the conception of increased excimer formation upon folding. The conclusions that can be extracted from the CD data are

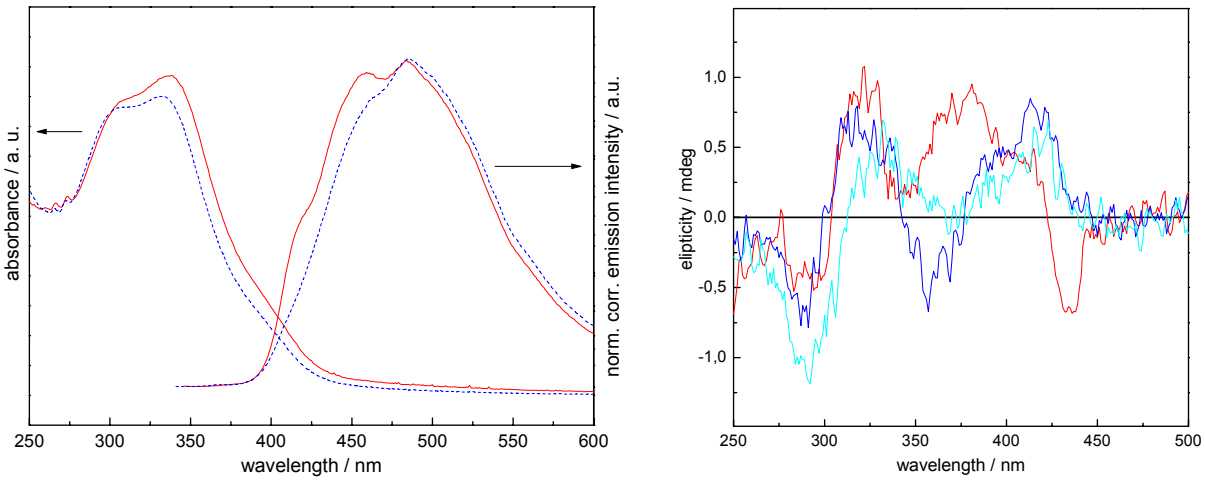

*Figure 20: Left: Absorbance and emission spectra of polymer **76** in chloroform (solid red) and acetonitrile (dashed blue). Right: CD spectra in chloroform (red), acetonitrile (blue), and acetonitrile:water = 90:10 mixture (cyan). Absorbance and CD were recorded at OD = 1 and emission at OD = 0.1.*

venturous. Although a trend is observed when going from chloroform to acetonitrile-water mixtures, absolute intensities are low. Probably the side chain does not induce enough chirality due to a poor order among the side chains themselves.

2.8 References

[1] U. H. F. Bunz, *Chem. Rev.* **2000**, *100*, 1605-1644; C. Weder (Ed.), *Adv. Polym. Sci.*, "Poly(arylene ethynylene)s: From Synthesis to Application", *Vol. 177*, Springer, Berlin, **2005**.

[2] D. Zhao, J. Moore, *Chem. Commun.* **2003**, 807-818.

[3] J. Li, Y. Pang, *Synth. Met.* **2004**, *140*, 43-48.

[4] Y. Pang, J. Li, T. J. Barton, *J. Mater. Chem.* **1998**, *8*, 1687-1690.

[5] D. Winter, C. D. Eisenbach, *J. Polym. Sci., Part A: Polym. Chem.* **2004**, *42*, 1919-1933.

[6] D. L. Trumbo, C. S. Marvel, *J. Polym. Sci., Part A: Polym. Chem.* **1986**, *24*, 2311-2326.

[7] S. Anderson, *Chem. Eur. J.* **2001**, *7*, 4706-4714.

[8] J. C. Nelson, J. G. Saven, J. S. Moore, P. G. Wolynes, *Science* **1997**, *277*, 1793-1796.

[9] K. Matsuda, M. T. Stone, J. S. Moore, *J. Am. Chem. Soc.* **2002**, *124*, 11836-11837.

[10] H. Goto, J. M. Heemstra, D. J. Hill, J. S. Moore, *Org. Lett.* **2004**, *6*, 889-892.

[11] H. Abe, N. Masuda, M. Waki, M. Inouye, *J. Am. Chem. Soc.* **2005**, *127*, 16189-16196.

[12] D. Zhao, J. S. Moore, *J. Am. Chem. Soc.* **2002**, *124*, 9996-9997.

[13] M. T. Stone, J. S. Moore, *J. Am. Chem. Soc.* **2005**, *127*, 5928-5935.

[14] X. Yang, L. Yuan, K. Yamato, A. L. Brown, W. Feng, M. Furukawa, X. C. Zeng, B. Gong, *J. Am. Chem. Soc.* **2004**, *126*, 3148-3162.

[15] 10.1002/chem.200501564 A. Khan, S. Hecht, *Chem. Eur. J.* **2006**, *12*, 4764-4774.

[16] L. Arnt, G. N. Tew, *Macromolecules* **2004**, *37*, 1283-1288.

[17] M. R. P. C. Tan, M. E. Kose, I. Ghiviriga, K. S. Schanze,, *Advanced Materials* **2004**, *16*, 1208-1212; X. Zhao, K. S. Schanze, *Langmuir* **2006**, *22*, 4856-4862.

[18] A. Khan, S. Hecht, *Chem. Commun.* **2004**, 300-301.

[19] M. J. Mio, L. C. Kopel, J. B. Braun, T. L. Gadzikwa, K. L. Hull, R. G. Brisbois, C. J. Markworth, P. A. Grieco, *Org. Lett.* **2002**, *4*, 3199-3202.

[20] D. T. McQuade, A. E. Pullen, T. M. Swager, *Chem. Rev.* **2000**, *100*, 2537-2574.

[21] K. Maeda, K. Morino, E. Yashima, *Macromol. Symp.* **2003**, *201*, 135-142.

[22] N. Kiriy, E. Jaehne, H.-J. Adler, M. Schneider, A. Kiriy, G. Gorodyska, S. Minko, D. Jehnichen, P. Simon, A. A. Fokin, M. Stamm, *Nano Lett.* **2003**, *3*, 707-712.

[23] J. R. Matthews, F. Goldoni, A. P. H. J. Schenning, E. W. Meijer, *Chem. Commun.* **2005**, 5503-5505.

[24] A. Khan, S. Hecht, *J. Polym. Sci., Part A: Polym. Chem.* **2006**, *44*, 1619-1627.

[25] R. A. Blatchly, G. N. Tew, *J. Org. Chem.* **2003**, *68*, 8780-8785.

[26] M. S. Wong, J.-F. Nicoud, *Tetrahedron Lett.* **1994**, *35*, 6113-6116.

[27] T. V. Jones, M. M. Slutsky, R. Laos, T. F. A. De Greef, G. N. Tew, *J. Am. Chem. Soc.* **2005**, *127*, 17235-17240.

[28] R. H. Grubbs, D. Kratz, *Chem. Ber.* **1993**, *126*, 149-157.

[29] S. Shotwell, P. M. Windscheif, M. D. Smith, U. H. F. Bunz, *Org. Lett.* **2004**, *6*, 4151-4154.

[30] A. Orita, E. Alonso, J. Yaruva, J. Otera, *Synlett* **2000**, 1333-1335.

[31] C. A. Hunter, K. R. Lawson, J. Perkins, C. J. Urch, *J. Chem. Soc., Perkin Trans. 2* **2001**, 651-669.

[32] H.-A. Klok, G. Kreutzer, N. Franz, *Synlett* **2006**, 1793-1815.

[33] N. I. Foster, N. D. Heindel, H. D. Burns, W. Muhr, *Synthesis* **1980**, 572-573.

[34] Z. Wu, J. S. Moore, *Tetrahedron Lett.* **1994**, *35*, 5539-5542.

[35] T. W. Greene, P. G. M. Wuts, *Protective Groups in Organic Synthesis*, 3rd ed., Wiley, New York, **1998**.
[36] R. B. Merrifield, *J. Am. Chem. Soc.* **1963**, *85*, 2149-2154.
[37] S. Takahashi, Y. Kuroyama, K. Sonogashira, N. Hagihara, *Synthesis* **1980**, 627-630; E.-I. Negishi, L. Anastasia, *Chem. Rev.* **2003**, *103*, 1979-2017.
[38] C. Amatore, A. Jutand, *Acc. Chem. Res.* **2000**, *33*, 314-321.
[39] B. Liang, M. Dai, J. Chen, Z. Yang, *J. Org. Chem.* **2005**, *70*, 391-393.
[40] J. Cheng, Y. Sun, F. Wang, M. Guo, J.-H. Xu, Y. Pan, Z. Zhang, *J. Org. Chem.* **2004**, *69*, 5428-5432.
[41] J.-H. Li, Y. Liang, Y.-X. Xie, *J. Org. Chem.* **2005**, *70*, 4393-4396.
[42] L. Wang, P. Li, Y. Zhang, *Chem. Commun.* **2004**, 514-515.
[43] 10.1002/ange.19590711102 L. Horner, E. H. Winkelmann, *Angew. Chem.* **1959**, *71*, 349-365.
[44] M. L. Gross, D. H. Blank, W. M. Welch, *J. Org. Chem.* **1993**, *58*, 2104-2109.
[45] The complete reaction mixture excluding TMSA was submitted to freeze-pump-thaw-cycles, and subsequently TMSA, where nitrogen was bubbled through for several minutes, was added.
[46] D. Coulson, *Inorg. Synth.* **1971**, *13*, 121-124.
[47] J. P. Rabe, S. Buchholz, *Science* **1991**, *253*, 424-427.
[48] The chiral side chain 2-(S)-methyl tetraethylene glycol monomethylether alcohol was provided by Christain Kaiser and derives from alanine.
[49] D. J. Gravert, K. D. Janda, *Chem. Rev.* **1997**, *97*, 489-509; P. H. Toy, K. D. Janda, *Acc. Chem. Res.* **2000**, *33*, 546-554.
[50] T. J. Dickerson, N. N. Reed, K. D. Janda, *Chem. Rev.* **2002**, *102*, 3325-3343.
[51] R. Duncan, *Nature Rev. Drug Disc.* **2003**, *2*, 347-360.
[52] J. C. Nelson, J. K. Young, J. S. Moore, *J. Org. Chem.* **1996**, *61*, 8160-8168.
[53] S. Chan, C. Yick, H. Wong, *Tetrahedron* **2002**, *58*, 9413-9422; P. Ashton, U. Girreser, D. Giuffrida, F. Kohnke, J. Mathias, F. Raymo, A. Slawin, J. Stoddart, D. Williams, *J. Am. Chem. Soc.* **1993**, *115*, 5422-5429.
[54] D. Twiss, R. Heinzelmann, *J. Org. Chem.* **1950**, *15*, 496-510.
[55] P. Reddy, S. Kondo, T. Toru, Y. Ueno, *J. Org. Chem.* **1997**, *62*, 2652-2654.
[56] H. Vorbrüggen, *Acc. Chem. Res.* **1995**, *28*, 509-520.
[57] T. Sasaki, K. Minamoto, H. Itoh, *J. Org. Chem.* **1978**, *43*, 2320-2325.
[58] R. Sinkeldam, M. van Houtem, G. Koeckelberghs, J. Vekemans, E. Meijer, *Org. Lett* **2006**, *8*, 383-385.
[59] G. C. Look, M. M. Murphy, D. A. Campbell, M. A. Gallop, *Tetrahedron Lett.* **1995**, *36*, 2937-2940.
[60] For example: L. Bi, M. Zhao, C. Wang, S. Peng, *Eur. J. Org. Chem* **2000**, *2669*, 2676.
[61] For example: F. Charvillon, R. Amouroux, *Tetrahedron Lett.* **1996**, *37*, 5103-5106.
[62] T. Nagamitsu, T. Sunazuka, H. Tanaka, S. Omura, P. Sprengeler, A. Smith, *J. Am. Chem. Soc.* **1996**, *118*, 3584-3590; H. Wang, I. Kozekov, T. Harris, C. Rizzo, *J. Am. Chem. Soc* **2003**, *125*, 5687-5700.
[63] M. Sanchez, T. Parella, E. Cervello, C. Jaime, A. Virgili, *Magn. Reson. Chem* **2000**, *38*, 925-931.
[64] S. Krishnamurthy, *Tetrahedron Lett.* **1982**, *23*, 3315-3318; H. Brown, P. Heim, *J. Org. Chem.* **1973**, *38*, 912-916.